UiT The Arctic University of Norway

Faculty of Science and Technology

Department of Geosciences

The Roles of Light Absorbing Particles in the Norwegian Arctic Snow

Olasubomi Quadri Olanrewaju

Master´s Thesis in Geology [GEO-3900]

May, 2023

ABSTRACT

Light absorbing particles (LAPs) such as black carbon (BC) and dust can reduce snow albedo and have a positive radiative forcing. Previous studies investigating LAP in snow in Tromsø focused on black carbon (BC) also called elemental carbon because it has human sources, but dust should also be considered because, while largely from natural sources, it is present in higher concentrations. To quantify the relative contribution of dust and BC in snow albedo reductions, snow samples were collected in Tromsø (Fjellheisen and Ekrehagen), Norway during the winter season from December 2022 to March 2023, both from surface snow and vertical profiles through the snow column. The samples were analyzed for particle concentration using gravimetric filtration, which provides a proxy of dust deposition. Snow reflectance was measured at both sites using a spectroradiometer to estimate the variation in snow reflectance from both sites. The SNICAR snow albedo model was used to evaluate the relative contribution of BC and dust to albedo reductions. The results from this study show that snow melt during warm periods, long dry periods of little additional accumulation of snowfall and wind all increase particle concentration in the surface layer of snowpack. Fresh snowfall generally has low gravimetric particle concentration. Snow particle concentrations are higher at Ekrehagen (70 m a.s.l.) than Fjellheisen (420 m a.s.l.) due to the 350 m elevation difference of the two sites. Ekrehagen has a higher occurrence of melt and rain, both of which increase particle concentrations, while Fjellheisen receives more snow and has a lower occurrence of times when particle concentrations are high on the surface of the snowpack. This has implications under a changing climate. As climate warms, more areas are more likely to get more rain and to have higher particle concentration surfaces, resulting in lower albedo, greater energy absorption, more melt of the snowpack and more energy kept in the Earth System. The SNICAR modeled spectral snow albedo indicates that dust is a greater driver of albedo reduction than BC. In both winter and spring dust only scenarios lower albedo more than BC only scenarios. However, the combination of BC and dust results in a further lower albedo reduction, but dust is the LAP that is most driving albedo reductions in the snow, with larger albedo reductions in late spring than in winter. The SNICAR modeled spectral snow albedo shows that 22% to 26% more of the incoming solar energy is being absorbed by the snowpack in spring relative to winter and contributing to melt. This is a large change in the surface energy balance. Therefore, it is important to include dust in analyses of LAP induced albedo reductions in snow.

ACKNOWLEDGMENT

First, I would like to thank my main supervisor Professor, Dr. Susan Kaspari from Central Washington University, USA for all the guidance, read throughs, motivation, and the privilege to write my master´s thesis under her supervision. I would also like to thank my co-supervisor Professor, Dr. Anders Schomacker from UiT The Arctic University of Norway who gave me valuable guidance in writing this thesis.

I am extremely grateful to the Norwegian government, for the opportunity given to me as an international student to study in Norway for free.

Finally, a big thank you to my friends and family members for their encouragement and moral support throughout my studies. Most importantly, I return all glory, honor and adoration to God almighty for seeing me through the course of my master´s study in Norway.

CHAPTER 1. INTRODUCTION AND LITERATURE REVIEW

1.1 Introduction

The Arctic is warming up to four times faster than the rest of the world (Rantanen et al., 2022). This phenomenon is known as Arctic or polar amplification. It is evident in both instrumental observations and climate models as well as in paleoclimate proxy records (Rantanen et al., 2022). The potential causes of Arctic amplification have been explained by several factors over the past decade, including increased oceanic heating and ice-albedo feedback due to declining sea ice (e.g., Screen et al., 2010; Jenkins & Dai, 2021), Planck feedback (Pithan & Mauritsen, 2014), lapse-rate feedback (Stuecker et al., 2018), near-surface air temperature inversion (Bintanja et al., 2011), cloud feedback (Taylor et al., 2013), ocean heat transport (Beer et al., 2020), and meridional atmospheric moisture transport (Graversen & Burtu, 2016) (Kim et al., 2017).

Impacts of Arctic amplification include decreased snow, glaciers, and sea ice, as well as an increase in precipitation falling as rain rather than snow. Aside from warming, another important factor driving snow and ice melt is the accumulation of Light Absorbing Particles (LAP) on snow such as dust, black carbon or microbial growth, that contribute to the snow and ice albedo feedback (Skiles et al., 2018). The presence of LAPs in snow reduces albedo (reflectivity) and increases the amount of solar energy absorbed by the snow, leading to earlier snowmelt and changes in the timing of seasonal runoff (Skiles et al., 2018).

Skiles et al. (2018) provide a review of the current understanding of LAP in snow globally, including their impact on the cryosphere and climate (Figure 1). This review summarizes the current understanding of the distribution of radiative forcing by LAPs in snow and discusses the obstacles that need to be overcome to limit global impacts, such as the limitations of local-scale observations, remote sensing technology, and the representation of LAP-related processes in Earth system models.

Overview of Snow Albedo

Snow serves as one of the primary barriers between the atmosphere and land surfaces while also being one of the most reflective surfaces on Earth. To understand the Earth's energy budget, snow is therefore a key factor. Albedo refers to how much of the sun's incoming light is reflected by a surface (Pedersen et al., 2015). The change in surface albedo which occurs due to fluctuations in temperature via snow and ice gain/loss have been long recognized to have a significant impact on climate change (Wexler, 1953). In the visible and near infrared spectrum (up to 1.4 μm, referred to as NIR), where the majority of the solar energy is available, snow is

a highly reflective medium (Warren, 1982). Snow is therefore a unique element of the climate system since snow-covered areas absorb less solar radiation than other surfaces like bare soil, vegetation, or oceans (Armstrong and Brun, 2008). A subsequent decrease in snow and ice cover as the climate warms shows a less reflective surface that absorbs more solar radiation, which amplifies the initial warming perturbation (Cess et al., 1991; Ingram et al., 1989; Robock, 1983; Schneider and Dickinson, 1974). Surface albedo feedback is the term for this positive feedback mechanism. At high latitudes, surface albedo feedbacks have long been associated with increased climate sensitivity (the response of the climate system to a given forcing) (Budyko, 1969; Sellers, 1969). The early energy balance models of Budyko (1969) and Sellers (1969) demonstrated that combination of planetary albedo and near-surface air temperature provides strong feedback between ice/snow and temperature when an external forcing (such as enhanced solar radiation) is applied (Thackeray & Fletcher, 2016).

Snow albedo in the visible region of the electromagnetic spectrum (400–700 nm) is mostly influenced by the number of particles present in the snow, with a minor/slight influence from the size of the snow grains. According to Wiscombe and Warren (1980) and Warren (1982), the size of the snow grains has a significant impact on snow's albedo in the infrared region of the solar spectrum (700-2500 nm) (Warren, 1982; Wiscombe and Warren, 1980; Skiles et al., 2018). Light absorbing particles (LAP; described further below) speed up melting by affecting snow albedo and the radiative forcing (RF) that results in increased solar irradiance absorption as a result of surface darkening. (Skiles et al., 2018). LAPs quickly reduce albedo across the visible wavelengths where snow is most reflective when at or near the snow surface.

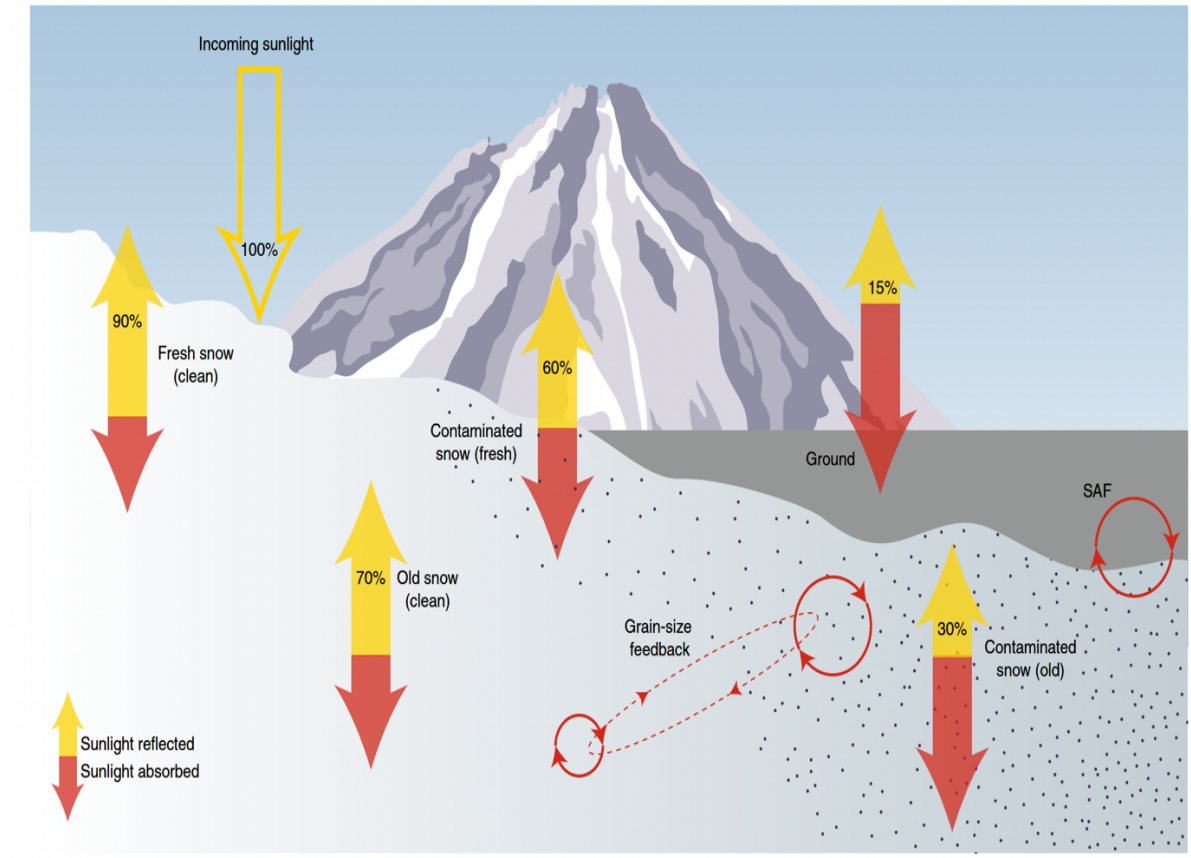

Figure 1. Light absorbing particles (LAP) impact on snow albedo and net solar radiation (from Skiles et al., 2018). The increased solar absorption caused by the presence of LAPs in snow is known as radiative forcing (RF). Red indicates absorption and yellow indicates reflection of incoming sunlight change with LAP content and snow age, which represents the snow grain size. The direct effect of LAPs (surface darkening) accelerates the aging of snow by promoting grain growth, which further reduces snow albedo (feedback from grain-size). Together, these two processes expedite melt, and when the snow cover quickly retreats, darker underlying surfaces (such the ground or ice) become more visible earlier, reducing the albedo at the landscape scale (SAF). Figure 2 shows variation in snow albedo across the range of snow reflectance for changing LAP content and snow grain size.

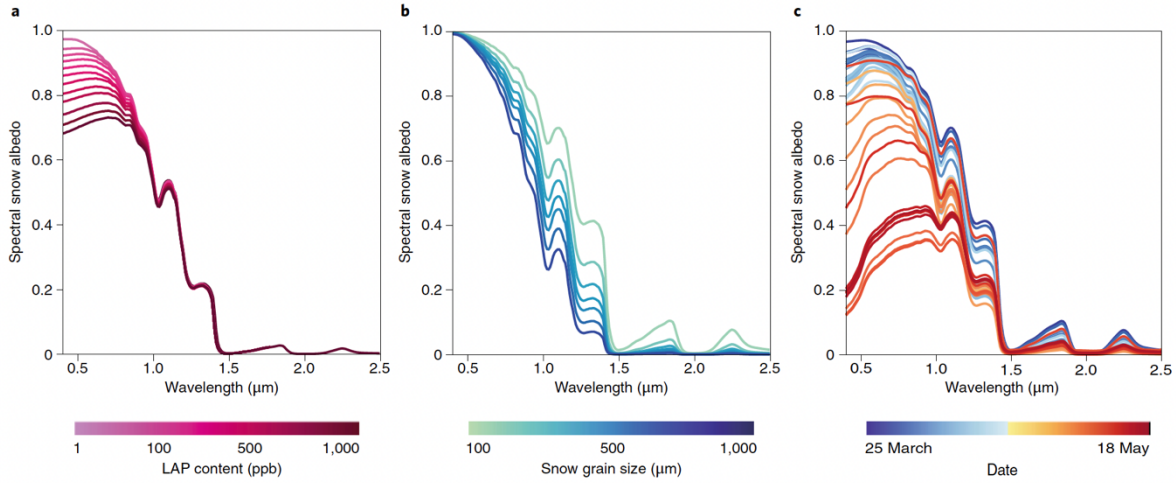

Figure 2. Variation in snow albedo across the range of snow reflectance for changing LAP content and snow grain size (from Skiles et al., 2018). (a) Snow albedo model demonstrating how visible albedo decrease as LAP content rises. (b) Clean snow model demonstrating decreasing snow albedo in the longer wavelength as snow grain size increases. (c) graph of daily time series of snow albedo declining during snowmelt, illustrating the combined effects of snow grain growth and LAP surface darkening.

Light Absorbing Particles (LAPs)

LAPs by definition absorb solar radiation, in contrast to light-scattering particles like sulfate aerosols which are responsible for cooling the atmosphere and the surface by reflecting sunlight or enhancing reflectivity (Charlson et al., 1992). LAPs in snow such as black carbon, mineral dust, and algae can influence snow albedo feedbacks, having a significant impact on the cryosphere and its evolution under a changing climate (Skiles et al., 2018). LAPs in the atmosphere trap solar radiation and heat up the absorbing aerosol layer. Depending on the vertical profile of LAPs in the atmosphere, the imposed heating may cause clouds to evaporate, increase or suppress vertical motions, and alter climate dynamics (Koch and Del Genio, 2010). Dry or wet deposition are both effective ways to remove these LAPs from the atmosphere (Bond and Bergstrom, 2006). On bright surfaces like snow, LAPs lower albedo after being deposited (Warren and Wiscombe, 1980). LAPs speed up the coarsening of the snow microstructure, which increases solar energy absorption and speeds up the intrinsic snow albedo feedback (Dumont et al., 2014).

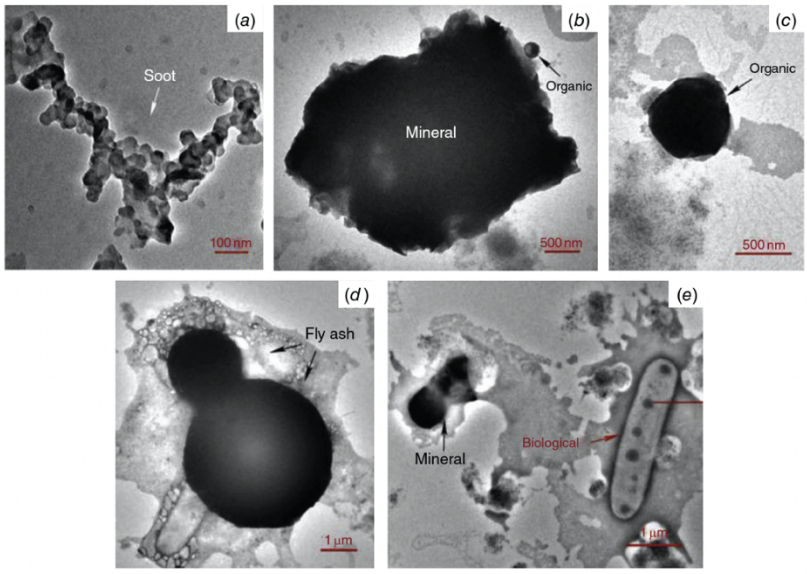

Figure 3. Demonstration of five different types of light-absorbing particles in snow obtained from transmission electron microscopy (TEM), including BC (a) mineral dust (b), brown carbon BrC (c), fly ash (d) and snow algae (e) (from Ren et al., 2017).

Black Carbon (BC)

According to Bond et al. (2004) and Stohl et al. (2013), black carbon (BC) particles are released into the atmosphere through incomplete burning from both anthropogenic (combustion engines, agricultural fires, domestic fireplaces and flaring) and natural sources (grassland and forest fires). BC is known to be a significant forcing agent in regional and global climate (Bond et al., 2013). The main sources of emission of BC differs by location. Approximately 60% of BC is released into the atmosphere by energy related combustion while the rest from biomass burning (Bond et al., 2013). BC is one of the main LAPs found in snow. (Bond et al., 2013). BC is a special type of carbonaceous aerosol that substantially absorbs across the visible and ultraviolet (UV) wavelength bands; even a small amount of BC in snow can significantly reduce the snow albedo because ice is practically non-absorbing at these wavelengths (Warren and Wiscombe, 1980). As an atmospheric aerosol and an impurity in snow and ice, BC is an extremely effective light absorber that affects radiation budgets (Bond et al., 2013). The increased solar energy absorbed by BC in the snowpack accelerates the spring melt by enhancing snow grain growth (Flanner et al., 2007). Positive albedo feedback increases the impact of early ice and snow melting, which emphasizes the significance of light-absorbing pollutants. The effect of BC on snow was first accentuated by Warren and Wiscombe (1980, 1985) and it was later integrated in climate models by Hansen and Nazarenko (2004), who calculated the BC-in-snow/ice

radiative forcing in the Northern Hemisphere's climate. They found that BC deposited on snow and ice reduces the albedo of the surface, resulting in increased absorption of solar radiation and subsequent warming of the snow and ice.

Black Carbon (BC) and Elemental Carbon (EC)

Although EC and BC are frequently used interchangeably, operational definitions of elemental carbon (EC) and black carbon (BC) are determined by the measurement technique utilized (Watson et al., 2005). The recent discovery of light-absorbing carbon that is not black ("brown carbon, Cbrown") makes it necessary to reevaluate and redefine the substances that make up light-absorbing carbonaceous matter (LAC) in the atmosphere (Andreae & Gelencsér, 2006). The majority of EC and BC characterization entails collecting PM on filters and measuring the carbon content on the filter or the attenuation of light reflected from or transmitted through the filter (Watson et al., 2005). The particles dispersed on top of the filter and throughout the filter have different scattering and absorption characteristics as they are in the atmosphere. These techniques frequently produce biased light absorption coefficients (b_{abs}) (Horvath, 1993). Generally, it is agreed that EC is the significantly contributor to b_{abs} (e.g., Horvath, 1993; Watson, 2002). Because of conduction electrons connected to the graphitic structure, EC absorbs light. EC is, therefore, often referred to as BC (Watson et al., 2005). However, by using the appropriate quantitative method, black and elemental carbon are defined. Thermal methods describe the same chemical entity as elemental carbon, but optical methods depict black carbon.

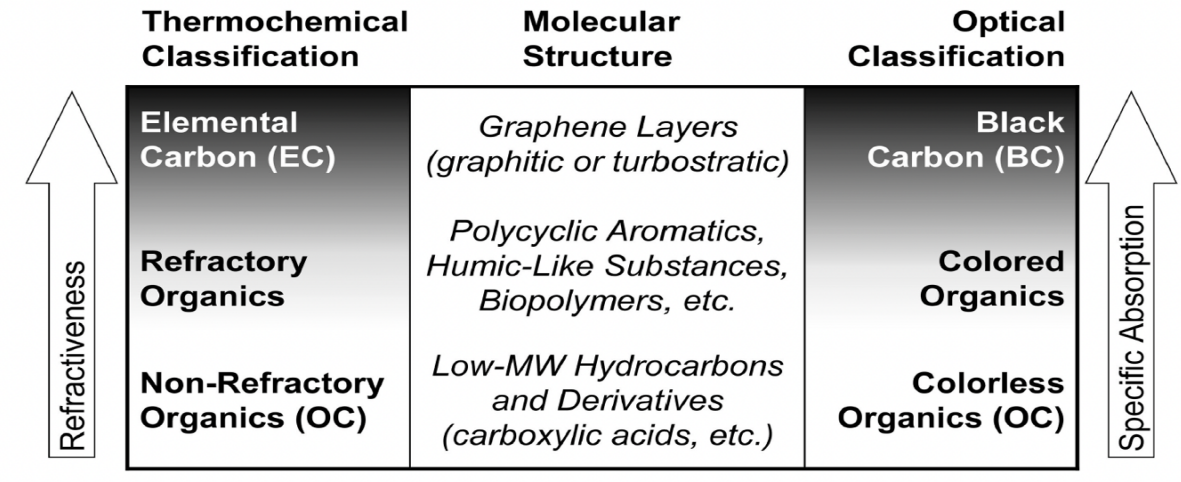

Figure 4. Classification and molecular structure of carbonaceous aerosol components (from Pöschl, 2003).

Sources of Black Carbon in snow in the Arctic

The sources of BC in the Arctic have undergone extensive research since the polar haze was first reported in 1956. Studies on BC in the Arctic troposphere using numerical models or back trajectory method have shown an anthropogenic origin, primarily from Europe and Russia in the winter (Polissar et al., 2001; Sharma et al., 2004, 2006; Stohl, 2006; Eleftheriadis et al., 2009; Hirdman et al., 2010). However, other studies (Bian et al., 2013; Liu et al., 2015; Qi et al., 2017a; Ikeda et al., 2017; Xu et al., 2017) suggested that Asian anthropogenic emissions were crucial, particularly in the middle and upper troposphere of the Arctic in springtime. Wang et al. (2014) suggested that around 50% of the BC loading in the Arctic came from Asia. Study from Koch and Hansen (2005) shows that the industrial emissions from southeast Asia were the largest BC sources for the Arctic due to the high industrial emission growth in southeast Asia and emission decline elsewhere. Other studies (Stohl, 2006; Bourgeois and Bey, 2011; Matsui et al., 2011) made the opposite argument due to the low transport efficiency of the Asain-Arctic transport pathway. Numerous case studies have shown that agricultural and boreal forest fires in central and western Eurasia may for a certain period of time, dominate the aerosol concentrations in significant portions of the Arctic troposphere in spring because many of the fires were burning at high latitudes at the time (Stohl et al., 2007; Treffeisen et al., 2007; Engvall et al., 2009; Warneke et al., 2009, 2010 (Matsui et al., 2013).

A recent study has shown that BC varies by source at surface in European and Siberian sectors of the Arctic (Qi et al., 2019). This validation was made feasible by a few recent studies using carbon isotope measurements (tagged tracer technique implemented in a 3D global chemical transport model GEOS-Chem), which distinguish the contribution of burning fossil fuels from burning biomass. The burning of fossil fuels was shown to be the primary cause of BC in Arctic surface air most of the time, while biomass burning predominates from April to September. However, the source of BC in the air is different from source of BC in the snow (Qi et al., 2019).

Sources of Black Carbon in the Air

The study from Qi et al. (2019) modeled BC sources (fossil fuel combustion versus biomass burning) using carbon isotope measurements at five different locations in the Arctic: Barrow (Alaska), Zeppelinfjellet (Svalbard), Abisko (Sweden), Alert (Canada) and Tiksi (Russia) (Figure 5). The model demonstrates that different Arctic sub-regions have distinct sources and source regions for BC in the troposphere, at the surface of the Earth, and in snow. The model accurately reproduces the reported annual mean fraction of biomass burning (fbb,%) at the five

locations to within 20%, and the predicted and observed monthly fbb values agree to within a factor of two. The results of the model point to fossil fuel combustion as the major source of BC in the troposphere (50-94%, vary with sub-regions), at the surface (55-68%), and in snow (58-69%) in the Arctic on an annual mean. However, biomass burning dominates at specific altitudes (600-800 hPa) and during specific times between April and September. Russian and European emissions, on the other hand, provide greater contributions to BC deposition than to BC in the atmosphere. Asian emissions from the combustion of fossil fuels account for the majority of BC loading in the Arctic sub-regions throughout both the winter (Oct.-Mar., 35-54%) and summer (Apr.-Sep., 34-56%). Siberian fossil fuel emissions are the major contributors to BC deposition in Russia both in the winter (62%) and the summer (46%), while European fossil fuel emissions are predominant in Ny-Ålesund (44% in the winter) and Troms (71% in the winter and 46% in the summer). For BC deposition in the North American sector, emissions from burning fossil fuels in Asia account for the majority of winter contributions (25–38%) and the majority of summer contributions (38–72%) (Qi et al., 2019).

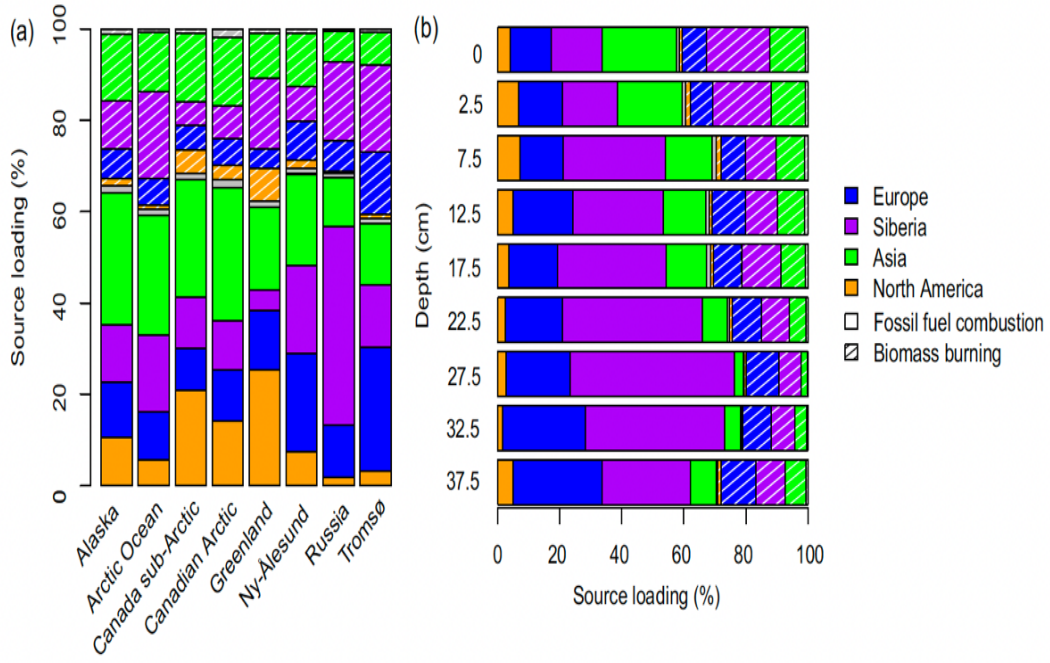

Figure 5. GEOS-Chem shows vertically varying sources and source regions of BC in different sub-regions in the Arctic. From Qi et al. (2019).

Other Light Absorbing Particles

Aside from BC, there are other types of light absorbing particles in snow that can reduce snow albedo, such as mineral oxides in dust, soil organics, volcanic ash, algae and other biological organisms and components (Skiles et al., 2018) (Fig. 3). For example, in Colorado (Painter et al., 2007), Inner Mongolia (Wang et al., 2013), and Japan (Aoki et al., 2006), mineral dust can dominate the light-absorption by LAPs on a regional scale, particularly in locations downwind of desert and semiarid regions. The most prevalent atmospheric aerosol, in terms of mass, is dust, which is produced by dry and semi-arid regions. Despite dust being a naturally occurring aerosol, new research has revealed that there has been a nearly doubling of atmospheric dust over the past century, most likely because of drought brought on by climate change and human land-use practices (Skiles et al., 2018). The light-absorbing component of primary organic carbon or secondary organic aerosols is referred to as brown carbon (BrC). Primary BrC is frequently present in soil (humic-like compounds (Dang and Hegg, 2014), plants, and other natural non-combustion sources, or it may be co-emitted with BC from combustion sources. The atmospheric transformation of organic species produces secondary BrC (Andreae and Gelencsér, 2006). BrC makes a less significant, but still considerable, impact to the decrease of snow-albedo (Wang et al., 2015).

Mineral dust (MD), one of the primary terrestrial producers of atmospheric aerosols, has a significant impact on regional and global climate by scattering and absorbing solar radiation, known as the direct radiative effect (Sokolik and Toon, 1996). Dust is likely to be discovered in snow cover that is downwind from substantial environments that have been subjected to disturbance. It is difficult to evaluate the global and regional effect of dust due to considerable variability in emission processes and the color and optical properties of dust that vary depending on the source region (Skiles et al., 2018). Mountain ranges in Europe are typically affected by Saharan dust deposition events, which make up 50–70% of the total annual dust deposition (Ginoux et al., 2001). In general, dust particles are larger compared to BC and they function as more efficient ice nuclei, with a better potential to affect cloud formation and precipitation (Creamean et al., 2013; Huang et al., 2014). As a result, they have a higher chance of mixing internally with ice grains. Moreover, dust has a relatively high mass abundance (ppm) in the snowpack, particularly in areas with seasonal and patchy snow cover or mountainous regions and can substantially reduce snow albedo and dominate light absorption (Painter et al., 2012; Di Mauro et al., 2015; Gabbi et al., 2015; Xie et al., 2018; Reynolds et al., 2020)

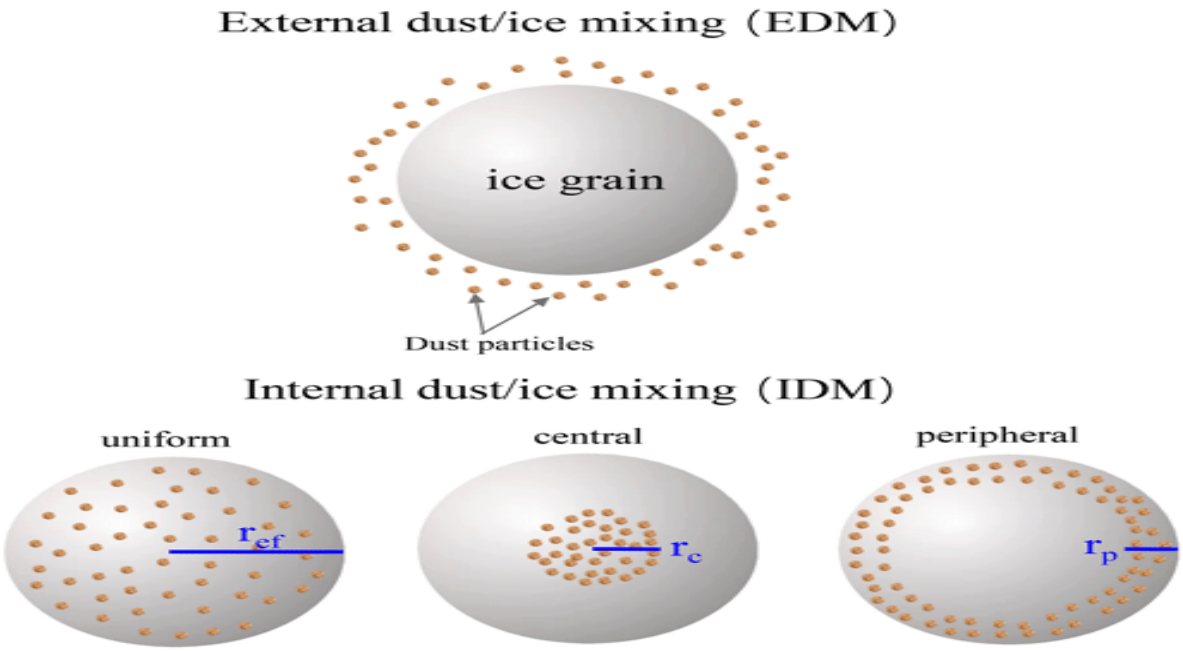

Figure 6. Schematic depicting various mixing scenarios of snow grains and dust particles. From Shi et al. (2021).

Mineral dust is a substantial light-absorbing aerosol that can potentially reduce snow albedo and enhance snow/glacier melting through wet and dry deposition on snow (Shi et al., 2021). To evaluate the impacts of mineral dust on absorption coefficient and albedo of the semi-infinite snowpack consisting of spherical snow grain, three scenarios of internal mixing of dust in ice grains were analyzed theoretically by combining asymptotic radiative transfer theory and (core-shell) Mie theory in Shi et al. (2021). The result from the study shows that internal dust-snow mixing significantly reduced snow albedo at a wavelength of <1.0 μm in general with bigger reductions at higher dust concentrations and larger snow grain sizes. Additionally, calculations revealed that a nonuniform distribution of dust in snow grains can result in considerable changes in the values of the absorption coefficient and albedo of dust-contaminated snowpack at visible wavelengths compared to a uniform distribution of dust in snow grains (Shi et al., 2021).

There has been a recent increased interest in light absorbing biological constituents in snow, a phenomenon that has only sporadically been investigated and quantified. Although snow is not often thought of as an ecological home, microbial life can exist there when liquid water, nutrients, and sunlight are available in appropriate quantities (Skiles et al., 2018). The most

well-known effect of snow microbes is the green – or pink – tinged "watermelon" snow. This is an effect caused by a community algae (of the genera Chloromonas, Chlainomonas and Chlamydomonas) as they evolve through various stages in their life cycle (Skiles et al., 2018). Algae can be brought in by atmospheric deposition or animal transport, and they can grow and concentrate on the surface of melting snowpacks or below it. Most likely, as a result of enhanced melting due to radiative forcing (RF) by algae, liquid water is produced and nutrients are released, which promotes additional algal growth in a positive feedback cycle (Skiles et al., 2018). The change in albedo are influenced by melt, the retreat of snowline, black carbon, dust and algae growth (Cook et al., 2020; Williamson et al., 2020; Box et al., 2012, 2017; Box, 2013; Tedstone et al., 2017, 2020; Ryan et al., 2019). Other studies have suggested a positive feedback mechanism between microbes, minerals and melting, where algae-induced melting releases ice-bound dust which in turn increases glacier algal blooms, leading to increased melting (Di Mauro et al., 2020; McCutcheon et al., 2021).

Processes affecting LAP concentrations in the snowpack

The concentration of all the mentioned LAP constituents (black carbon, mineral dust, soil organics, volcanic ash, algae, and other biological organisms and components) in surface snow is determined by their mixing ratio in precipitation (wet deposition), the quantity that is brought to the surface through dry deposition, mechanical mixing of local soils and other organic matter with the already-existing snowpack, biological growth in the snow, and impurity redistribution in the snowpack through post-depositional processes like wind-driven drifting, sublimation, and melt (Doherty et al., 2010). As was shown in some Arctic profiles in Doherty et al. (2010), vapor loss from the snowpack to the atmosphere via sublimation in winter can enhance concentrations of impurities at the top surface before the start of runoff. Changes in snow cover are significantly influenced by LAPs, particularly black carbon (BC), brown or organic carbon, mineral dust, and algae (Réveillet et al., 2022).

Impact of LAP on Earth Energy Balance and Water Resource

Light absorbing particles (LAPs) affect the Earth's energy balance and water resources. Wildfires in the snow zone have an impact on ablation by reducing snow albedo and increasing surface solar irradiance by removing forest canopy and depositing light absorbing particles such as black carbon on the snowpack which lowers snow albedo. Although little is understood on how variation in BC deposition impacts post-wildfire snowmelt timing, but very much relevant to water resources (Uecker et al., 2020). The study from Uecker et al. (2020)

shows that post wildfire has an important source of BC to the snowpack and the impact increases by an order of magnitute in regions of high versus low burn severity and decreased by two orders of magnitude over a decade. The seasonal distribution of water resources, regional hydrological cycles, and societal sustainable development are all impacted by changes in glacier/snow cover melting (Ramanathan and Carmichael, 2008; Xu et al., 2009; Sang et al., 2019). Snow albedo feedback is still one of the least understood concepts in regional and global climate modeling (He et al., 2018a; Skiles et al., 2018; IPCC, 2013) and calls for further research. This is due to differences in the amount and distribution of BC in snow and ice as well as variations in the size and mixing state of BC particles (He et al., 2018a; Schwarz et al., 2013).

1.2 LITERATURE REVIEW

Background on prior research investigating Light Absorbing Particles (LAP) in snow around Tromsø, Norway

Previous work has been done investigating LAP in Tromsø by Pedersen et al. (2015), Doherty et al. (2013), Qi et al. (2019), and Forsström et al. (2013) with a primary focus on black and elemental carbon.

Previous study done in Tromsø by Pedersen et al. (2015)

Pedersen et al. (2015) collected snow samples throughout the 2008-09 winter in Tromsø to investigate the impact of elemental carbon (EC) on snow and its corresponding spectral surface albedo reduction. The study used in-situ observations of EC in snow and corresponding measurements of spectral surface albedo reduction to examine the spatial and temporal patterns of EC deposition on snow surfaces (Table 1). Pedersen et al. (2015) also analyzed the relationship between EC concentrations and spectral surface albedo reduction to better understand the mechanisms of EC-induced snowmelt.

The EC concentrations in the snow were determined by analyzing the filters using a thermo-optical method with the Thermal/Optical Carbon Aerosol Analyzer (Sunset Laboratory Inc., Forest Grove, USA) and one of two different temperature protocols, the NIOSH (National Institute of Occupational Safety and Health) 5040 and the EUSAAR 2 (European Supersites for Atmospheric Aerosol Research) protocol (Birch, 2003; Cavalli et al., 2010; Forsström et al., 2009).

Site	Date of sample collection	Number of samples	Snow depth (cm)	EC Minimum (ng/g)	EC Maximum (ng/g)	EC Median (ng/g)	EC Mean (ng/g)	EC STD (ng/g)
Ramfjorden, Tromsø	03.04.2008	7	20 ± 1	10	27	13	17	6
Valhall, Tromsø	30.04.2008	3	66 ± 13	126	140	137	134	6
Met. no, Tromsø	07.02.2008 to 20.05.2008	15	55 ± 19	1	1542	85	277	446

Table 1. Summary of elemental concentrations (ng/g) in snow (from Pedersen et al., 2015).

Based on the research conducted by Pedersen et al. (2015), the snow samples collected in Tromsø have an EC concentration in the range 1 to 1543 ng/g and median of 66 ng/g. In Tromsø, there were two exceptionally high EC concentrations (1225 and 1543 ng/g) during two melting events in May 2009. The filters were heavily loaded at these occasions, which reduced the precision of the distinction between organic and elemental carbon (Cavalli et al., 2010). For these, the EC concentrations were estimated from the average ratio of EC to total carbon in all samples.

The primary finding of this investigation is the direct observation of a systematic decrease in snow albedo by EC. A broadband albedo loss of 0.004 is seen in comparison to clean snow at even ECequiv concentrations as low as 10 ng/g. Greater concentrations result in greater reductions, and, depending on the lighting circumstances, EC concentrations one order of magnitude higher correlate to an almost five-fold increase in albedo reduction.

Pederson et al. (2015) shows that EC was present in snow samples from all sites, and that the amount of EC was positively correlated with snow grain size. This research also measured the spectral reflectance of snow samples and found that the presence of EC caused a reduction in

albedo across all wavelengths. The reduction in albedo was particularly strong in the near-infrared portion of the spectrum, which has implications for the energy balance of the snowpack and the surrounding environment.

Previous study done in Tromsø by Doherty et al. (2013)

Doherty et al. (2013) collected snow samples on a mountain plateau (Fjellheisen) in Norway 69.5 N, 19.0 E) at an elevation of 420 m above and to the east of the town of Tromsø. Subsequently, snow was also collected in 2008 on this plateau on May 21, 23, 26, 28, and 30 as the snowpack was melting, with rain events on May 27 and 28. The purpose of Doherty et al. (2013) was to investigate the vertical distribution of black carbon (BC) and other insoluble light-absorbing particles (ILAPs) in snow and their impact on snow albedo and radiative forcing. The collected snow samples were filtered and use a specially designed spectrophotometer system to look at the absorption of the filter, and how it varies with wavelength. If it is dominated by black carbon absorption is constant across wavelengths, whereas if it is dominated by dust, it will be variable with wavelength. They estimated the concentrations based on filters that they have made with a known amount of BC.

Six consecutive days of measurements in Tromsø in 2008 reveal an increase in the quantities of light-absorbing particles in surface snow with melting (21–30 May). The average subsurface snow concentrations for each profile were used to derive amplification factors describing the higher insoluble light-absorbing particulates (ILAP and L) or BC (B) concentration in surface snow relative to concentrations in subsurface snow or in freshly fallen snow (A_L and A_B) respectively (Table 2). Key abbreviations and variables in Doherty et al. (2013) paper. ILAP : Insoluble light-absorbing particulates, L : Black carbon-equivalent mass concentration in snow (ng/g or ppb) of all ILAP in snow, based on total light absorption measured in the 650-700 nm wavelength range,B : Estimated black carbon concentration in snow (ng/g or ppb), made by assuming total absorption results from a linear combination of absorption by BC with $å_{abs}$, BC of 1.0 and non-BC constituents with $å_{abs}$, non-BC of 5.0, A_L, A_B : Amplification factor that describes the higher ILAP (L) or BC (B) concentration in surface snow relative to concentrations in subsurface snow or in freshly fallen snow. The concentration, called **L**, accounts for absorption by all ILAP, measured as the amount of black carbon that must be present to fully account for the absorption of all particles between 650 and 700 nm. An estimate of the BC concentration, B, is made by assuming total absorption results from a linear

combination of absorption by BC with $å_{abs}$, BC of 1.0 and non-BC constituents with $å_{abs}$, non-BC of 5.0 (Doherty et al., 2010).

Date	Total snow depth (cm)	Top 3 cm L*(ng/g)*	Subsurface L*(ng/g)*	Top 3 cm. B*(ng/g)*	Subsurface B *(ng/g)*	AL (Amplification factor)	AB (Amplification factor)
19.05.2008	27	16	19	14	17	0.9	0.9
21.05.2008	22	22	19	19	16	1.2	1.2
23.05.2008	22	49	20	44	18	2.4	2.5
26.05.2008	17	48	20	43	17	2.4	2.4
28.05.2008	30	72	23	64	19	3.1	3.3
30.05.2008	17	87	35	72	29	2.5	2.5

Table 2. Concentrations and amplification factors for all ILAP (L and AL, respectively) and for BC (B and AB) in the mountain snowpack near Tromsø, Norway in 2008 (from Doherty et al., 2013).

The results of Doherty et al. (2013) showed that black carbon and other insoluble light-absorbing particles are concentrated near the surface of the snowpack during melting, especially in Arctic regions. The average subsurface snow concentrations within each profile were used to compute the amplification factors (AL and AB). Similar to Barrow and Dye-2, as the snow melts, the surface snow concentrations increase (Doherty et al., 2013). By the end of the measurements, the amplification factors for the top 3 cm of the snowpack are around 2-3. Here, the abs in the layer of melt amplification show no discernible trend in $å_{abs}$, showing comparable scavenging rates for BC and non-BC ILAP. The result from Doherty´s research show that the concentration of BC and other insoluble light absorbing particulate in surface snow increase with melting because their scavenging efficiency with snow melt water is less than 100 percent.

This concentration near the surface leads to increased absorption of sunlight and warming of the snowpack, which can accelerate melting and reduce the snow cover duration. The study found that the concentration of black carbon and other insoluble light-absorbing particles varied widely depending on the location and season of year, with higher concentrations found in regions closer to industrial activity and biomass burning sources. The study also found that the vertical redistribution of these particles during melting can lead to their retention in the snowpack and eventual deposition on the underlying surface.

Previous study done in Tromsø by Qi et al. (2019)

Research by Qi et al. (2019) was done to assess sources of BC simultaneously in the atmosphere and in snow to analyze sources of BC between 2007 and 2009, a period during which both observations of BC concentration at the surface and in snow were available. Using a tagged tracer technique implemented in a global 3D chemical transport model called GEOS-Chem, BC sources in the troposphere, in surface air, and in snow in different seasons in the Arctic were systematically investigated. These investigations were constrained by both observations of BC concentrations and carbon isotope measurements (Qi et al., 2019).

To enable direct comparison with observations, Qi's study in GEOS Chem separated the contribution of combustion of biofuel from anthropogenic contributions (Table 3). First-time validation of the source apportionment simulation was done using carbon isotope data.

Fossil fuel combustion (a)

	ng m^{-2} day^{-1}	ng m^{-2} day^{-1}	ng m^{-2} day^{-1}	ng m^{-2} day^{-1}
	N. America	Europe	Siberia	Asia
Tromsø	134 (3)	3566 (71)	735 (15)	318 (6)

Biomass burning (b)

	ng m^{-2} day^{-1}	ng m^{-2} day^{-1}	ng m^{-2} day^{-1}	ng m^{-2} day^{-1}
	N. America	Europe	Siberia	Asia
Tromsø	313 (1)	157 (1)	199 (1)	1251 (4)

The numbers in parenthesis are relative contributions (%) from various sources.

Table 3. GEOS-Chem simulated BC deposition fluxes in the Arctic from Biomass burning from October to March averaged for 2007–2009 (ng m^{-2} day^{-1}) (from Qi et al., 2019).

The result of the Qi et al. (2019) investigation shows that the primary sources of BC in the Arctic were from incomplete combustion of biomass and fossil fuels, with biomass burning being the dominant source. Biomass burning, and Asian contributions are more significant in spring while fossil fuel combustion from Russia and Europe dominated BC in snow in the Arctic throughout the fall and winter. Qi et al. (2019) noted that the seasonal variation was due to the changing sources of atmospheric transport and weather conditions in the Arctic region. Overall, the study of Qi et al. (2019) research shows that, except for Russia and Tromsø, where contributions from Siberian and European emissions dominated respectively, Asian emissions were the major contributor of BC in snow across most of the Arctic sub-regions. Earlier

research concentrated on the sources of BC deposition in the Arctic rather than allocating sources of BC in snow, and they identified Siberian and European anthropogenic emissions as the two main contributors of BC in snow (Huang et al., 2010; Bourgeois and Bey, 2011; Sharma et al., 2013; Wang et al., 2014; Ikeda et al., 2017).

Previous study done in Tromsø by Forsström et al. (2013)

Forsström et al. (2013) collected snow samples from the snow surface as well as from vertical profiles in the snow column in Tromsø between 2007-08. The study aimed to determine the concentrations and seasonal variations of EC in Arctic snow from various locations in the European Arctic, as well as to identify potential sources of EC such as local combustion sources, long-range transport from other regions, or natural sources. Thermal optical analysis was used to determine the concentration of EC in the samples (Table 4).

Site	date	EC(ng/g)	sites	Subsite samples	description	latitude	longitude	altitude	*hSWE* *b(mm)*
Tromsø	10.01.2008 to 20.05.2008	*53.3 (31.3–95.1)*	1	*24 (86)*	town	*69.65*	18.94	94	178
Tromsø Ramfjorden	06.03.2007	5.4	1	1(1)	sea ice	69.52	19.23	0	*99 bE*

Table 4. Median elemental carbon concentrations (EC), with 25th and 75th percentiles in parentheses) from Tromsø and Tromsø Ramfjorden (from Forsström et al., 2013).

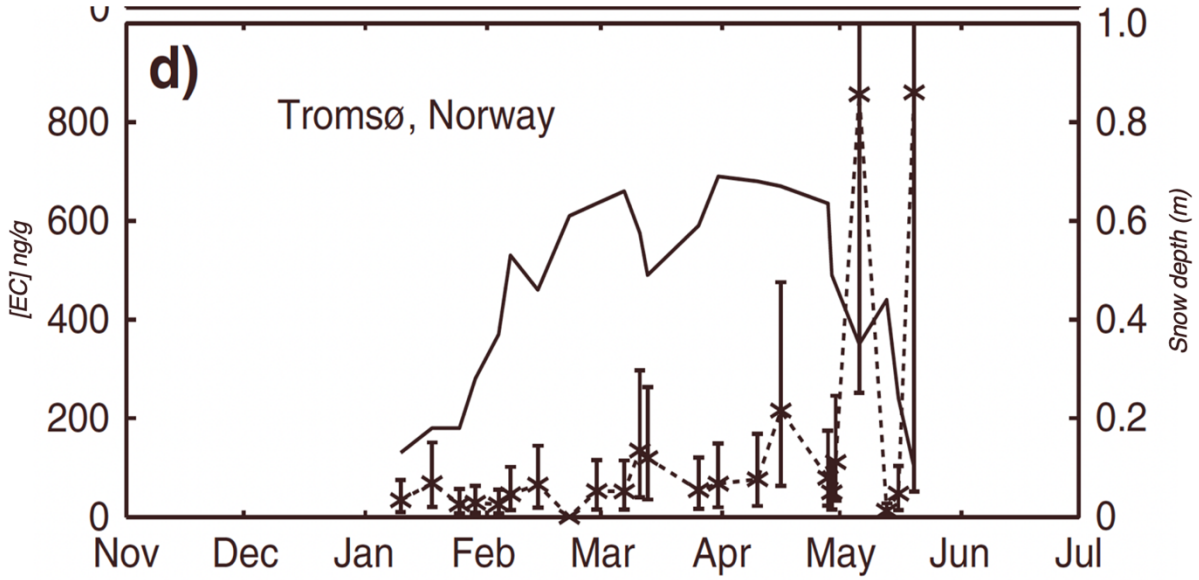

Fig. 7. Samples collected in an urban site near downtown Tromsø, at the instrument field of the Norwegian Meteorological Institute (100 m a.s.l.). At the three later sites snow depth (plotted as black (2008) was monitored throughout the sampling period, in Tromsø by manual measurements. From Forsström et al. (2013).

The Forsström et al. (2013) results show that in 2008, the snowpack in Tromsø began to rapidly melt in the final days of April, resulting in EC levels exceeding 800 ng/g; lower values later returned following a snow event in mid-May; and finally, another peak in concentrations appeared when melting picked up again. In both 2008 and 2009, a sharp decline in snow depth was followed by the highest surface EC concentrations ever recorded during the study. The result of this study demonstrates that at monitoring sites, around the start of snowmelt in April or May, 1-2 months after the annual peak in atmospheric concentrations, a rapid increase in EC concentrations in surface snow of up to an order of magnitude was seen (Figure. 6). Insoluble particles that are left at the surface as meltwater runs off are probably the cause of these increases, which normally occur at the same time as the start of rapid snowmelt.

SITE	Latitude	Longitude	Method	Date	BC (ng/g)	EC(minimum) (ng/g)	EC(maximum) (ng/g)	EC(median) (ng/g)	EC(mean) ng/g	Study
Tromsø	69.65	18.94	Thermal Optical Method	10.01.2008 to 20.05.2008	-	-	31.3 – 95.1	53.3		Forsström et al., 2013
Tromsø Ramfjorden	69.52	19.23		06.03.2007	-	5.4	-	-		
Fjellheisen	69.5	19.0	Integrating-sandwich spectrophotometer	19.05.2008	0.9	-	-	-		Doherty et al., 2010
				21.05.2008	1.2	-	-	-		
				23.05.2008	2.5	-	-	-		
				26.05.2008	2.4	-	-	-		
				28.05.2008	3.3	-	-	-		
				30.05.2008	2.5	-	-	-		
Ramfjorden Tromsø	69.54	19.18	Thermal Optical Method	03.04.2008		10	27	13	17	Pederson et al., 2015),
Valhall Tromsø	69.66	18.95		30.04.2008		126	140	137	134	
Met. No Tromsø	69.65	18.93		07.02.2008 to 20.05.2008		1	1542	85	277	

Table 5. Summary of research in Tromsø by Pedersen et al. (2015), Doherty et al. (2013), Qi et al. (2019) and Forsström et al. (2013) with a primary focus on black and elemental carbon.

Based on the prior four studies done in Tromsø (Table 5), the current knowledge indicates that black carbon (BC) and other insoluble light-absorbing particles are present in the snowpack in Tromsø, a town located in the Arctic region of Norway. Doherty et al. (2013) observed that black carbon was redistributed vertically within the snowpack during the melting season, indicating that the black carbon particles were present at various depths in the snowpack. The vapour loss from snowpack into the atmosphere by the process of sublimation can cause enhancement of concentration at the surface of snowpack. When black carbon and other

insoluble light-absorbing particles are deposited on the surface of snow, they can be subjected to mechanical trapping. This occurs when the particles are trapped within the ice crystals that form as the snow melts and refreezes. As the snow melts, the ice crystals form channels that can trap particles and prevent them from sinking into the snowpack. These particles can percolate within the snowpack with melt water. Pederson et al. (2015) found that the presence of black carbon in the snow causes a reduction in spectral surface albedo, which in turn can contribute to increased melting. The study's key finding is the direct observation of BC's systematic lowering of snow albedo. A broadband albedo loss of 0.004 is seen even at ECequiv concentrations as low as 10 ng /g when compared to clean snow. Qi et al. (2019) studied the sources of black carbon in the atmosphere and in snow in the Arctic and found that it can be transported over long distances and deposited in remote regions. The study also reported that black carbon concentrations in snow were highest during winter and spring. Qi et al. (2019) identified both atmospheric and local sources of black carbon in the Arctic, with local sources being the dominant contributors. Forsström et al. (2013) measured elemental carbon in European Arctic snowpacks and found that black carbon levels were higher in the late winter and early spring, suggesting that seasonal variations play a role in the amount of black carbon present in snow. In general, the current knowledge from all four studies suggests that black carbon is present in the snowpack in Tromsø and varies seasonally, with higher concentrations during the melting season. The sources of black carbon are diverse and include both local and long-range transport. The presence of black carbon in snow can have significant impacts on the albedo and melting of the snowpack.

The research on LAP that were earlier conducted by Doherty and Pedersen in Arctic Norway was primarily focused on black carbon, with little research on dust and light absorbing organics. Boy et al. (2019) discuss the need for more comprehensive LAP research in Arctic Norway, noting that dust, particularly from northern high latitudes, has received little attention. Previous research hypothesize that dust has the same impact on the cryosphere as black carbon, but not enough research has been conducted to experiment and prove this. There has not been enough research done in Arctic Norway to test the hypothesis that dust has the same effect on the cryosphere as black carbon. However, my thesis research will help to close this information gap.

CHAPTER 2. METHODOLOGY

2.1 Sampling Site

Snow samples were collected at two different locations, Fjellheisen (on a mountain plateau) located 420 m above sea level, which is to the east of the city of Tromsø, Norway (69.5° N, 19.0° E) and Ekrehagen at 70 m above sea level (69.6° N, 18.9° E), which is on Tromsøya.

A suitable site was selected at each location for sampling to ensure that sampled snow is in-situ and not altered by local human activities. Fjellheisen was accessed by cable car, a four to five minutes trip with the cable car from the lower station (near sea level) to the upper station called Storsteinen. The upper station is not a developed site, but it´s a popular destination, which offers tourists an enjoyable view of the city and the surrounding islands and fjords.

At Fjellheisen, sampling was conducted 1 km to 1.7 km away from the cable car, in undisturbed areas with minimal vegetation. Sometimes, it was not possible to sample in the exact same location due to human disturbance of snowpack. Therefore, a nearby new sampling site with no human influence was selected for sampling.

Ekrehagen is located near the ski jumps and 200 m away from the road, with a pond and meadow surrounded by forest, and is one of the more remote locations on Tromsøya. This site was selected to allow background LAP levels on Tromsøya to be determined. The sampling site was never altered by human activities, although there were times when ski tracks were spotted near the sampling site as a groomed cross country ski route was near the sampling site.

Figure 8. Map of the study area (Google Earth).

Figure 9. Fjellheisen sampling site (March 4, 2023).

Figure 10. Ekrehagen sampling site (February 24, 2023).

2.2 Sampling method

A surface snow sample was collected with a clean stainless-steel shovel from the upper 2 cm of the snow (1.5 to 4.5 kg) in a Whirl-Pak bag and labelled “surface sample”. The shovel was used to dig the snowpit to the ground level and snowpack depth was measured. The shovel was used to collect a vertical column of snow (1.5 to 4.5kg) from the bottom of the snowpack to the surface in a Whirl-pak bag and labelled “column sample”. All samples collected in Whirl-Pak bags were double bagged in case of leakage. Additionally, surface samples and column samples were collected in 50 mL centrifuge vials which will be analyzed later in 2023 for black carbon (BC) via a Single Particle Soot Photometer at Central Washington University in the United States of America.

All snow samples were transported frozen to the freezer outside Naturfagbygget building at UiT and kept frozen in the freezer until sample analysis. Samples for gravimetric filtration were brought out of the freezer and placed in a clean container to melt 24 hours prior to gravimetric filtration.

Figure 11. Surface sample collection at Ekrehagen (December 12, 2022).

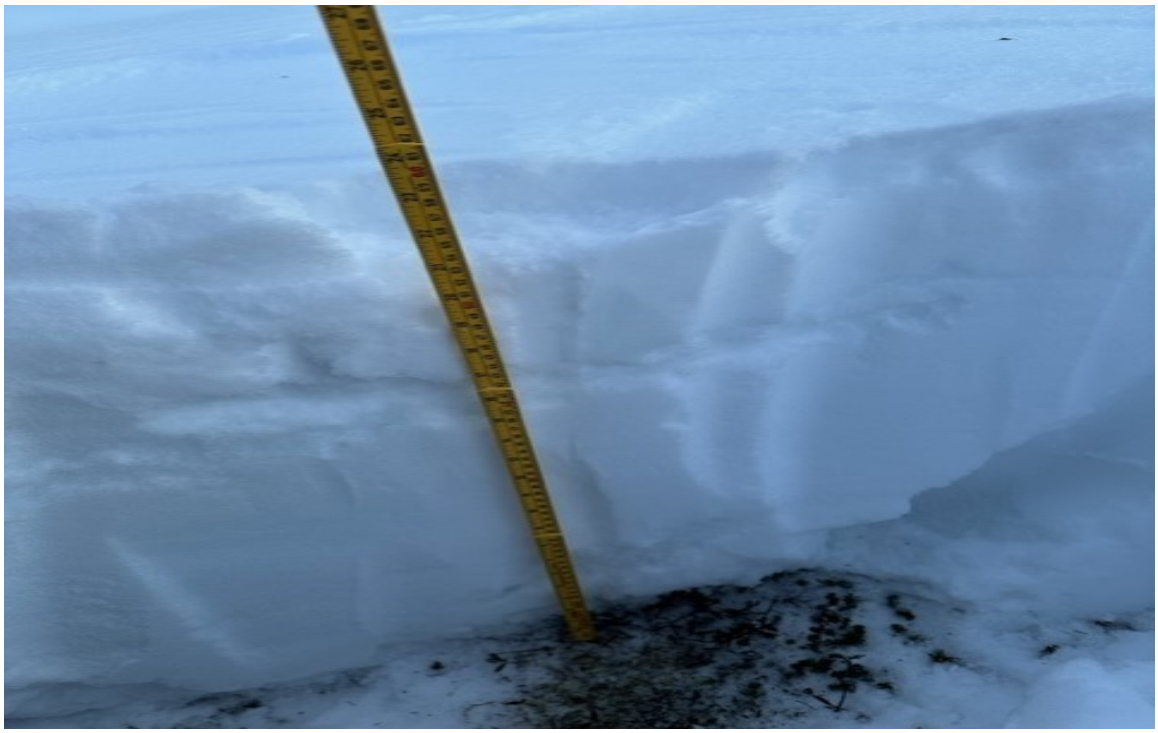

Figure 12. Vertical column section of snowpack from ground level to snow surface at Ekrehagen (December 12, 2022).

2.2 Snow gravimetric sample filtration

2.2.1 Filter preparation procedure

Millipore 47 mm diameter 0.45 μm cellulose filters manufactured were used to filter the samples, and plastic petri dishes (LOT 218807095) (PN 7231) were used to store the filters (1 per filter). The weighing balance was powered on a few minutes before use. Filters were handled using forceps. It usually takes up to a minute for the weighing balance to register the weight correctly. The weight of each filter was recorded (out to the fourth decimal place = 0.0000 g) in a notebook, and the filter was stored in a petri dish. Three to four standard filters were regularly weighed as a "method blank" to ensure the measured filter mass was reproducible. The mass of filters was first measured at the Arctic University Museum of Norway using an Ohaus balance. Later filter mass was measured using a Sartorius balance at the laboratory at the Department of Geosciences, UiT The Arctic University of Norway on March 21, 2023.

Filters initially measured at the Arctic University Museum of Norway were re-measured at the laboratory to check the consistency in the measurements between the two balances; the difference ranged between 0.0001 to 0.0002 g.

Figure 13. Weighing filters at the Arctic University Museum of Norway.

2.2.2 Filtration

All the snow samples collected in the Whirl-Pak bags were removed from the freezer and placed in a clean container at room temperature for snow to melt prior to gravimetric filtration. A balance with a 1g precision was used to weigh the mass of each snow sample with the Whirl-Pak bag on it and then the mass was recorded in a notebook. The pre-weighed filter was gently placed on the clean filter apparatus using forceps in the center of the filtration apparatus and secured using a magnetic clamp. The pre-weighed filter was wet with MQ water. The pump was turned on to ensure that the desired flask can be vacuumed. The melted snow in the Whirl-Pak bag was then poured into the funnel, maintaining liquid in the funnel while also swirling the sample in Whirl-Pak bag to ensure all particles ended up on the filter. When particles remained in the Whirl-Pak bag, the bag was rinsed with MQ water and poured into the filter funnel. After the entire sample was filtered, the pump was turned off, the funnel cup was carefully taken off, and the forceps were used to remove the filter and gently place it back in the corresponding petri dish. Thereafter, the filtration apparatus was rinsed with MQ water

before another sample was filtered. The mass of the Whirl-Pak bag was then weighed and recorded in a notebook.

Figure 14. Sample filtration in the laboratory.

2.2.3 Drying filters

After each filter was placed in its corresponding petri dish, the upper cover of the dish was set in such a way that the dish was not tightly closed. The filter (in a petri dish) was then placed in a fume hood and was allowed to dry overnight at room temperature. After 24 hours of drying, the petri dish was shut and closed tightly. An image of each filter was taken after drying to document the particle load (Figure 16 and Figure 17).

2.2.4 Determining Particle Concentration

Dried filters were weighed again using the same procedure as before the filtration process. The new weight was then recorded in a notebook. The weight (after filtration) was subtracted from the old weight (before filtration) to get the weight of particle mass in each sample. The weight of each particle was divided by the mass of each sample collected from the field to give particle

concentration in g/g. Particle concentration in g/g was multiplied by 1,000,000 to give particle concentration in µg/g.

2.3 SNICAR Snow Albedo Modeling

Snow albedo was modeled using SNICAR-ADv3: Online Snow Albedo Simulator (http://snow.engin.umich.edu/) inputs assuming diffuse incident radiation; sub-Arctic winter surface spectral irradiance conditions; 1 meter snowpack thickness; 200 kg/m^3 snowpack density; Picard et al. (2016)/Warren and Brandt (2008) ice refractive index data; 100 µm snow grain effective radius; hexagonal plates (aspect ratio of 2.5) snow grain shape; 0.25 broadband albedo of underlying ground; sulfate-coated black carbon concentration (nanograms); dust concentrations evenly distributed across size bins 2, 3 and 4; sahara (Balkanski et al., 2007) dust type; to stimulate this model.

2.4 Snow reflectance

Snow spectral reflectance was measured using a Spectral Evolution PSR+3500 Portable Spectroradiometer (spans 350-2500 nm) with an 8° lens, and output was based on ten scans. Reflectance was calibrated using a 99% Spectralon diffuse reflectance standard.

CHAPTER 3. RESULTS

3.1 Snow depth and snow classification

Snow samples were collected during the winter period in 2022-23 at Fjellheisen and Ekrehagen (Table 6) in various sample conditions (fresh, aged, wind crust and rainy).

Date	Time	Location	Coordinates (North and East)	Snow depth (cm)	Sample condition (surface snow)
07.12.2022	10:30AM	FJELLHEISEN	69.6345523, 18.9942046	20	FRESH
07.12.2022	12:00PM	EKREHAGEN	69.6868777, 18.9579197	7	FRESH
12.12.2022	12:38PM	EKREHAGEN	69.6868677, 18.9579197	12.5	FRESH
13.12.2022	10:45AM	FJELLHEISEN	69.6328502, 18.9933306	23	FRESH
16.12.2022	10:54AM	EKREHAGEN	69.6885263, 18.9580686	27	WIND CRUST
17.12.2022	01:00PM	FJELLHEISEN	69.6328502, 18.9933306	43	FRESH
09.01.2023	12:20PM	EKREHAGEN	69.6885263, 18.9580686	44	FRESH
11.01.2023	10:46AM	FJELLHEISEN	69.6322038, 18.9951863	90	AGED
14.01.2023	12:53PM	EKREHAGEN	69.6906301, 18.9634776	56	FRESH
18.01.2023	11:54AM	FJELLHEISEN	69.6620741, 18.9797458	36	AGED

21.01.2023	12:22PM	EKREHAGEN	69.6980644, 18.9706822	53	FRESH
25.01.2023	12:40PM	FJELLHEISEN	69.6395531, 18.9492833	32	WIND CRUST
26.01.2023	10:55AM	EKREHAGEN	69.6906301, 18.9634776	63	WIND CRUST
31.01.2023	01:10PM	FJELLHEISEN	69.6322038, 18.9951863	84	FRESH
02.02.2023	11.12AM	FJELLHEISEN	69.6308036, 18.9945325	67	FRESH
06.02.2023	12:14PM	EKREHAGEN	69.6865758, 18.9579375	71	HEAVY RAIN
16.02.2023	11:18AM	EKREHAGEN	69.6906301, 18.9634776	55	AGED
22.02.2023	11:59AM	FJELLHEISEN	69.6308076, 18.9942325	24	FRESH
24.02.2023	12:34PM	EKREHAGEN	69.6867604, 18.9579157	75	FRESH
28.02.2023	10:49AM	EKREHAGEN	69.6867403, 18.9583002	76	(RAINY/FRESH)
04.03.2023	10:43AM	FJELLHEISEN	69.6346672, 18.9945111	40	FRESH
08.03.2023	11:56AM	FJELLHEISEN	69.6347500, 18.9941030	51	FRESH
10.03.2023	02:14PM	EKREHAGEN	69.6867889, 18.9580196	131	FRESH

15.03.2023	12:22PM	FJELLHEISEN	69.6345207, 18.9941500	42	FRESH
16.03.2023	11:11AM	EKREHAGEN	69.6866347, 18.9580833	141	FRESH
21.03.2023	11:15AM	FJELLHEISEN	69.6347871, 18.9939491	56	FRESH
22.03.2023	10.18AM	EKREHAGEN	69.6866817, 18.9577819	161	FRESH
29.03.2023	13:53AM	FJELLHEISEN	69.6310909, 18.9954153	123	FRESH
29.03.2023	15:08PM	EKREHAGEN	69.6866010, 18.9580320	140	FRESH

Table 6. Data for sample collection at Fjellheisen and Ekrehagen during the 2022-2023 winter (December 7, 2022 – March 29, 2023).

Figure 15 shows variation in snow depth over time at Ekrehagen and Fjellheisen for 2022-2023 winter. Variation in snow depth between Ekrehagen and Fjellheisen was due to change in sampling site as discussed earlier in Chapter 2, the sampling site at Fjellheisen was changed frequently due to human influence. For this reason, the snow depth pattern at Fjellheisen does not follow the same trend as Ekrehagen.

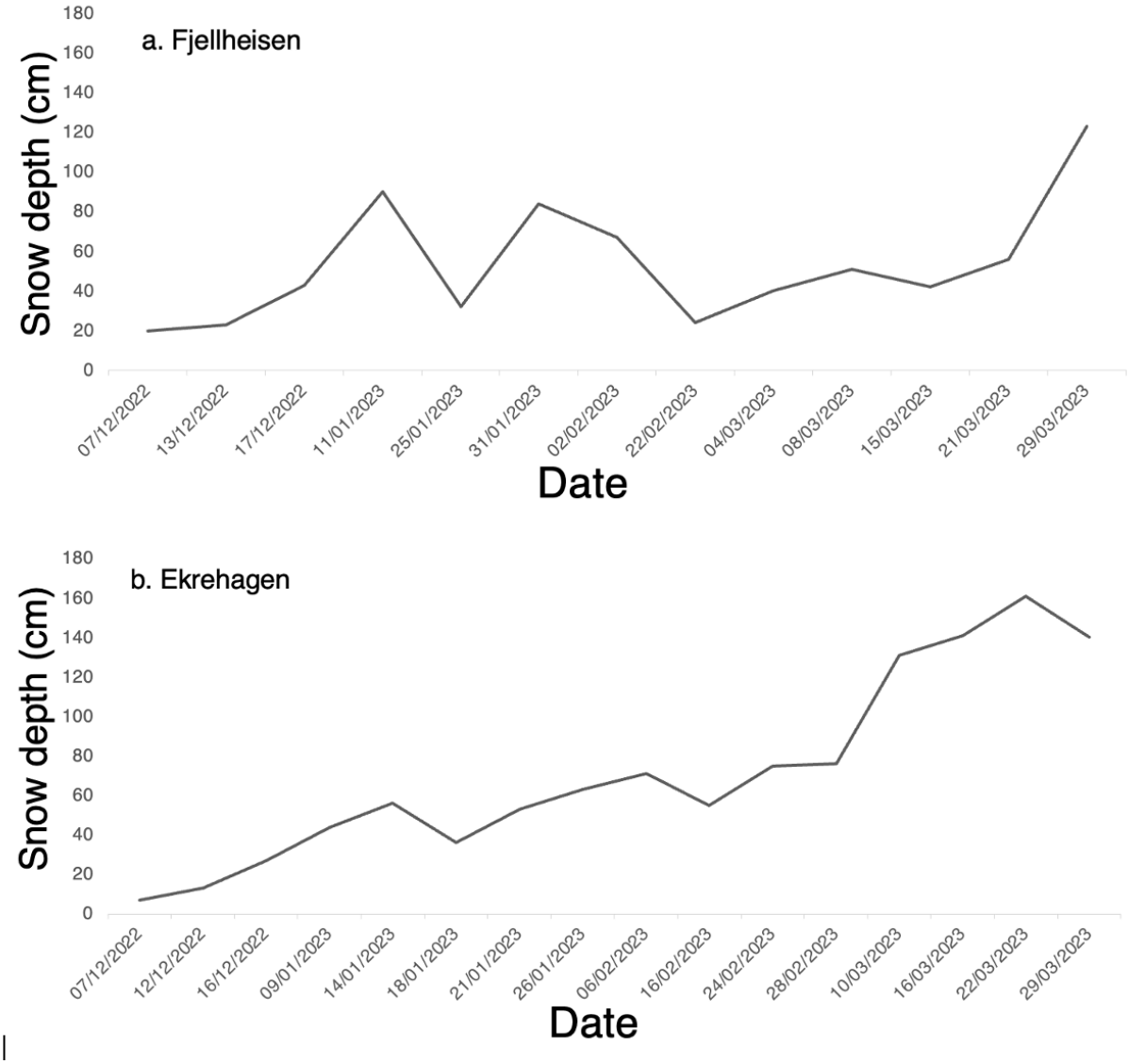

Figure 15. Graph of snow depth (cm) plotted against date for (a) Fjellheisen, and (b) Ekrehagen.

Snow depth for each site increases over the winter (Figure 15) except for when it does not snow for a couple of days (usually 2- 4 days) or when temperatures are positive. During these situations the sample condition is recorded as “aged snow”. There are occasions where the recorded snow depth at Fjellheisen decreases even when it snows, primarily because the sampling site was changed due to observation of human influence at the sampling site and secondarily due to wind scavenging. Snow samples collected during the period of December to early January were of low density (fresh snow). During the month of February, sampling was done twice only at Fjellheisen as most of the snow had been affected by rain at Ekrehagen.

Snow samples collected during rainy days are categorized as “rainy” (either aged or fresh), while the samples collected when windy are categorized as “wind crust”.

3.2 Impact of Large Organic Matter on Particle Concentration

After gravimetric filtration in the laboratory, large visible organic matter (such as plant leaves and roots) was observed on some of the filters from Ekrehagen (EK) and Fjellheisen (FJ). This organic material may have been transported into the snowpack by wind. Based on the size of the material seen on the filters, it originated quite locally, was not transported very far, and is heterogeneous in the snowpack. This larger material is of less interest from a snow albedo perspective because it has a low surface area relative to its mass and is not an effective absorber of sunlight compared to the smaller particles that have high surface area to mass. To quantify how the large organic matter (LOM) contributes to particle concentration on the filters, each filter with large organic matter was weighed and recorded. Thereafter, forceps were used to remove all visible large organic matter from the filter and re-weighed (Table 7). The surface sample collected from the upper 2 cm of snow are surface snow, while the vertical column of the snowpack are column samples.

Sample	Date	Filter #	Mass of particle (g) without LOM	Mass of particle (g) with LOM	Particle concentration (µg/g) without LOM	Particle concentration (µg/g) with (LOM)
BLANK		1	0	0	0.00	0.00
BLANK		2	0	0	0.00	0.00
EKSURFACE	12.12.2022	3	0.0234	0.0256	9.42	10.31
EK COLUMN	14.01.2023	4	0.0133	0.0142	2.99	3.20
FJ COLUMN	18.01.2023	5	0.0004	0.0208	0.11	5.97
EK COLUMN	12.12.2022	6	0.0061	0.0336	2.29	12.61

FJ SURFACE	11.01.2023	7	0.0297	0.0412	6.98	9.68
FJ SURFACE	13.12.2022	8	0.003	0.0089	0.90	2.67
FJ SURFACE	17.12.2022	9	0.0005	0.0011	0.21	0.45
FJ COLUMN	17.12.2022	10	0.0005	0.0005	0.24	0.24
FJ COLUMN	11.01.2023	11	0.003	0.0039	0.81	1.05
EK COLUMN	21.01.2023	12	0.0083	0.0163	2.16	4.23
EK SURFACE	21.01.2023	13	0.001	0.0016	0.39	0.62
EK COLUMN	09.01.2023	14	0.0062	0.0076	1.95	2.39
EK SURFACE	14.01.2023	15	0.002	0.0032	1.41	2.25
EK COLUMN	16.12.2022	16	0.0016	0.0023	0.70	1.01
EK AGED SNOW	14.01.2023	17	0.0066	0.0109	1.88	3.10
EK SURFACE	18.01.2023	18	0.0002	0.0002	0.07	0.07
EK SURFACE	16.12.2022	19	0.0012	0.0021	0.88	1.55
FJ SURFACE	25.01.2023	20	0.0017	0.0024	0.62	0.88
FJ COLUMN	13.12.2022	21	0.0034	0.0089	1.07	2.81

FJ COLUMN	25.01.2023	22	0.0284	0.0485	6.33	10.81
EK SURFACE	09.01.2023	23	0.0489	0.0505	19.12	19.74
FJ COLUMN	07.12.2022	24	0.0081	0.0081	3.76	3.76
EK SURFACE	26.01.2023	25	0.0002	0.0002	0.09	0.09
EK COLUMN	26.01.2023	26	0.0105	0.0141	2.37	3.18
FJ SURFACE	31.01.2023	27	0.0001	0.0001	0.06	0.06
FJ FRESH SNOW	31.01.2023	28	0.001	0.001	0.55	0.55
FJ AGED SNOW	31.01.2023	29	0.0222	0.0334	5.12	7.70
FJ SURFACE	07.12.2022	30	0.0019	0.003	0.86	1.36
EK SURFACE	07.12.2022	31	0.0028	0.0035	1.57	1.97
EK COLUMN	07.12.2022	32	0.0028	0.0039	1.31	1.82
FJ SURFACE	02.02.2023	33	0.0002	0.0007	0.09	0.32
FJ FRESH SNOW	02.02.2023	34	0.0012	0.0012	0.62	0.62
FJ COLUMN	02.02.2023	35	0.0077	0.0105	2.19	2.99
EK COLUMN	06.02.2023	36	0.0058	0.0065	1.56	1.75

EK SURFACE	06.02.2023	37	0.0052	0.0162	1.55	4.84
EK COLUMN	16.02.2023	38	0.0091	0.0091	2.13	2.13
EK SURFACE	16.02.2023	39	0.0631	0.0631	16.28	16.28
FJ COLUMN	22.02.2023	40	0.0023	0.0023	0.66	0.66
FJ SURFACE	22.02.2023	41	0.0002	0.0002	0.09	0.09
EK SURFACE	24.02.2023	42	0.0001	0.0001	0.08	0.08
EK FRESH SNOW	24.02.2023	43	0.0001	0.0001	0.06	0.06
EK AGED SNOW	24.02.2023	44	0.0201	0.0201	5.77	5.77
EK SURFACE	28.02.2023	45	0.0027	0.0027	1.26	1.26
EK COLUMN	28.02.2023	46	0.0141	0.0141	3.47	3.47
FJ SURFACE	04.03.2023	47	0.0002	0.0002	0.07	0.07
FJ COLUMN	04.03.2023	48	0.0053	0.0053	1.72	1.72
FJ SURFACE	08.03.2023	49	0.0009	0.0009	0.37	0.37
FJ COULMN	08.03.2023	50	0.0011	0.0011	0.34	0.34
EK SURFACE	10.03.2023	51	0.0016	0.0016	0.86	0.86

EK COLUMN	10.03.2023	52	0.0094	0.0094	2.04	2.04
FJ COLUMN	15.03.2023	53	0.0035	0.0035	0.91	0.91
FJ SURFACE	15.03.2023	54	0.0007	0.0007	0.38	0.38
EK SURFACE	16.03.2023	55	0.0001	0.0001	0.06	0.06
EK COLUMN	16.03.2023	56	0.0092	0.0092	2.24	2.24
FJ SURFACE	21.03.2023	57	0.0007	0.0007	0.28	0.28
FJ COLUMN	21.03.2023	58	0.0009	0.0009	0.18	0.18
EK SURFACE	22.03.2023	59	0.0001	0.0001	0.06	0.06
EK COLUMN	22.03.2023	60	0.0069	0.0069	1.81	1.81
FJ SURFACE	29.03.2023	61	0.0014	0.0014	0.54	0.54
FJ COLUMN	29.03.2023	62	0.0018	0.0018	0.41	0.41
EK SURFACE	29.03.2023	63	0.0131	0.0131	4.82	4.82
EK COLUMN	29.03.2023	64	0.0121	0.0121	2.75	2.75

Table 7. Particle concentration for samples with visible large organic matter (LOM) and the particle concentration after LOM was removed.

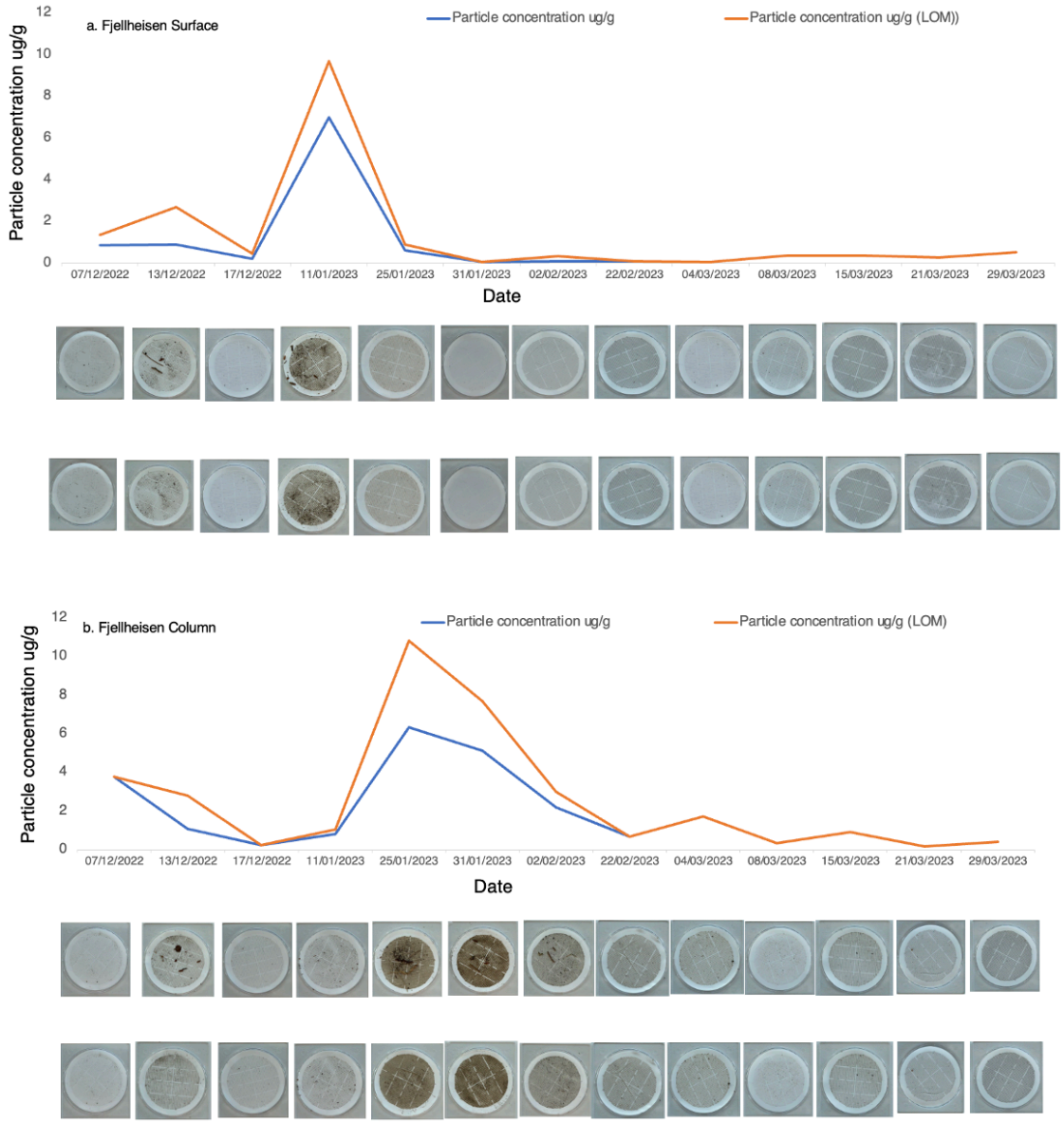

Figure 16. Graph of particle concentration with large organic matter (LOM) vs particle concentration without LOM for Fjellheisen (a) surface and (b) column. Images on the top row are filters with LOM and the images on the bottom row are filters without LOM.

For Fjellheisen surface, only filters from December 13, 2022, December 11, 2022, January 5, 2023, January 11, 2023, and February 2, 2023 had large organic matter removed from them; the rest of the filters do not contain LOM. For Fjellheisen column, only filters from December 13, 2022, January 11, 2023, January 25, 2023, January 31, 2023 and February, 2023 had large organic matter removed from them; the rest of the filters do not contain LOM.

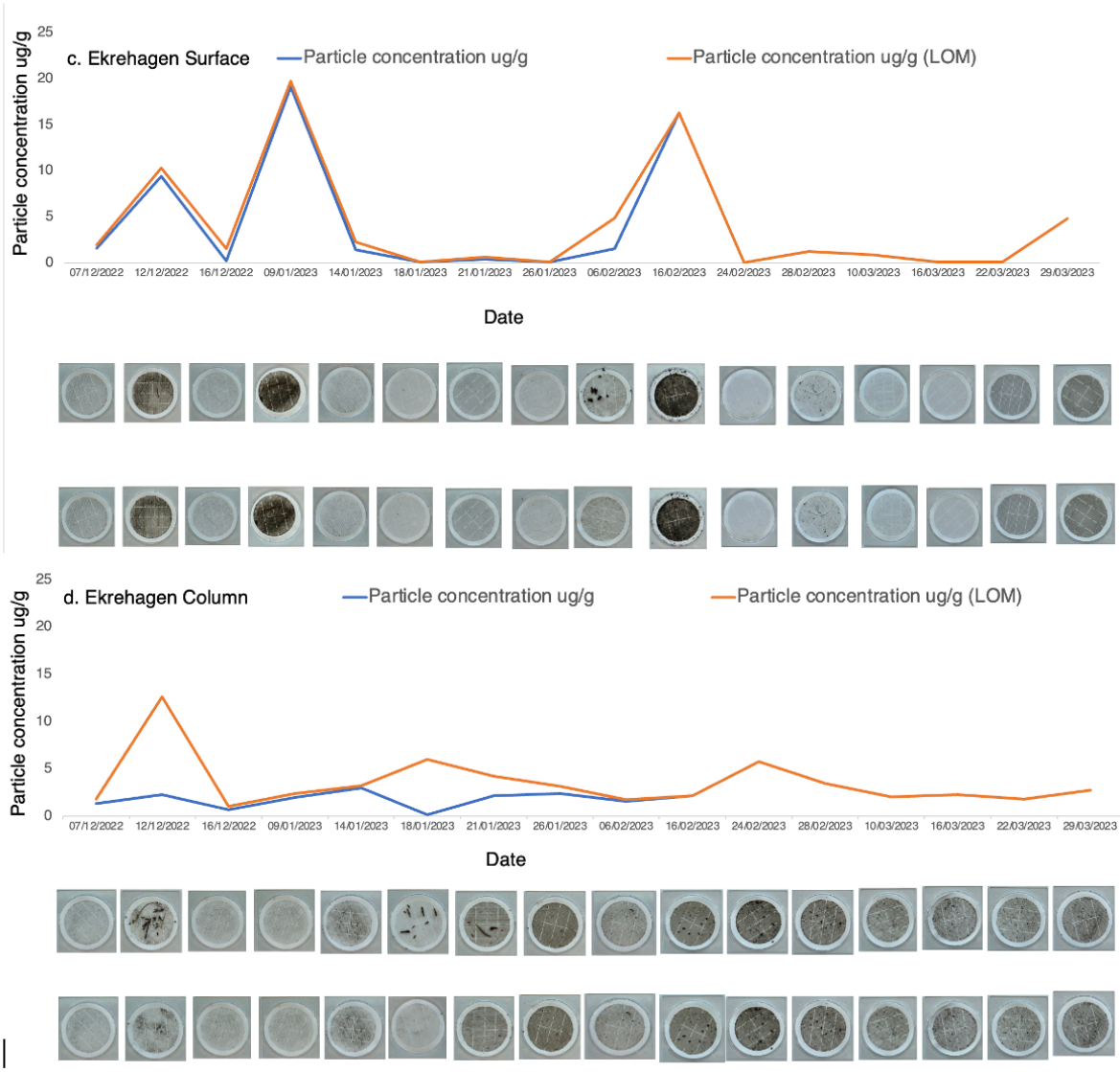

Figure 17. Graph of particle concentration with large organic matter (LOM) vs particle concentration without LOM for Ekrehagen (c) surface and (d) column. Images on the top row are filters with LOM and the images on the bottom row are filters without LOM.

For Ekrehagen surface, only filters from December 12, 2022, December 14, 2022, December 16, 2022, January 9, 2023, and February 6, 2023 had large organic matter removed from them; the rest of the filters do not contain LOM. For Ekrehagen column, only filters from December 12, 2022, December 18, 2022, January 21, 2023 and January 26, 2023 had large organic matter removed from them; the rest of the filters do not contain LOM.

3.3 Summary of Particle Concentration in Snow at Ekrehagen and Fjellhesien

Table 8 summarizes the minimum, maximum, average and mean particle concentration without LOM for Ekrehagen and Fjellheisen.

Site	Number of observations	Minimum (µg/g)	Maximum (µg/g)	Average (µg/g)	Mean (µg/g)
FJ Surface	13	0.06	6.98	0.88	0.37
FJ Column	13	0.18	6.33	1.83	0.91
EK Surface	16	0.06	19.12	3.62	1.07
EK Column	16	0.11	5.77	2.23	2.14

Table 8. Summary of particle concentration (µg/g) at Fjellheisen and Ekrehagen without LOM.

After filters with LOM were removed, particle concentration without LOM was plotted against date for (a) Fjellheisen surface (b) Fjellheisen column (c) Ekrehagen surface (d) Ekrehagen column (Figure 18) to see how particle concentration varies with time.

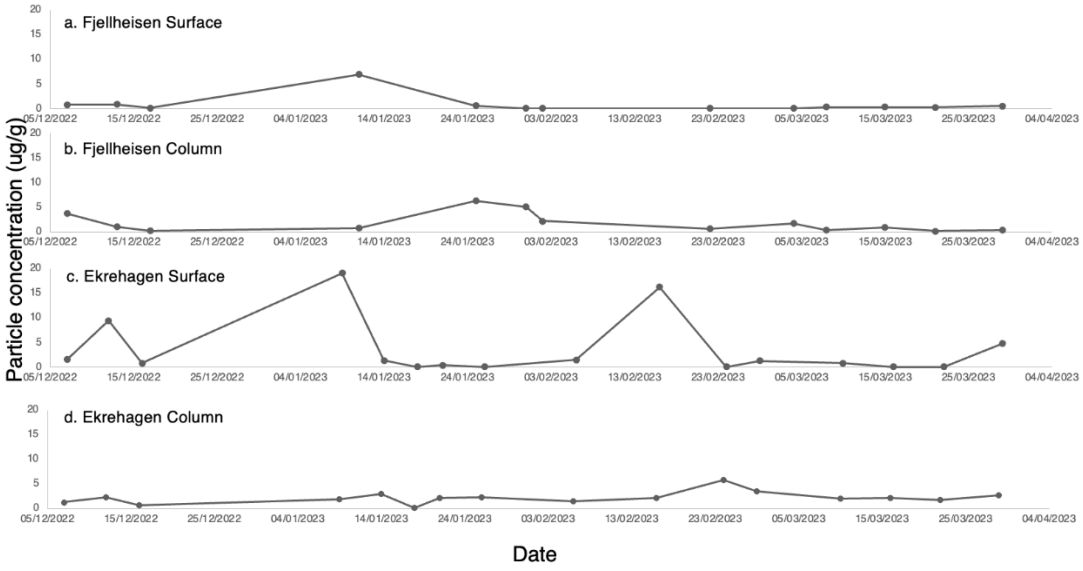

Figure 18. Graph of particle concentration without LOM (a) Fjellheisen surface, (b) Fjellheisen column, (c) Ekrehagen surface and (d) Ekrehagen column.

3.4 Snow Reflectance

On March 29, 2023, snow reflectance was measured at Fjellheisen and Ekrehagen using a spectroradiometer (Figure 19). The missing data on the graph were removed due to noise from the detector.

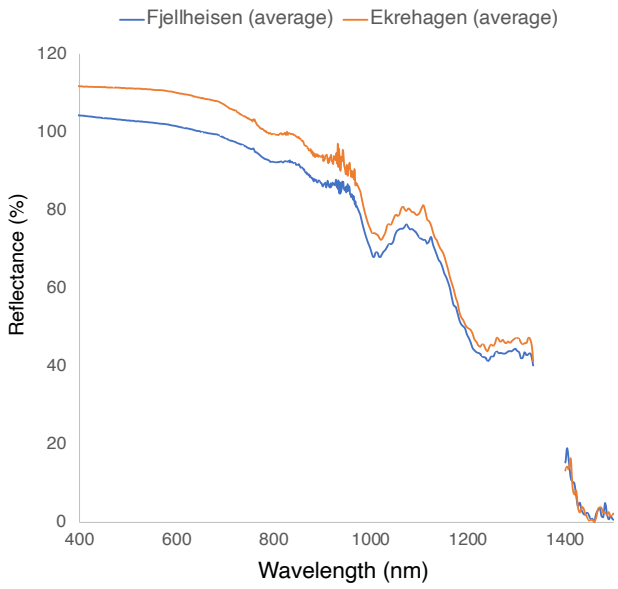

Figure 19. Variation in snow reflectance at Fjellheisen (blue line) and Ekrehagen (orange line).

Figure 20. Snow surface at (a) Fjellheisen and (b) Ekrehagen with spectralon reference standards (the white standard is 99% reflective, the black is 1% reflective).

CHAPTER 4. DISCUSSION

4.1 Variation in particle concentration between Fjellheisen surface and column

The particle concentration in Fjellheisen column layer tends to be higher than the surface layer (Table 8). For the whole season, the mean particle concentration is higher in the column layer than the surface layer (0.91 μg/g and 0.37 μg/g respectively).

To understand variability in particle concentration between the surface layer and column layer over time, meteorological data including snow depth, precipitation (24 hr), average of mean wind speed from main observations (24 hr), minimum air temperature (24 hr) and maximum temperature (24 hr) (Figure 21) from Tromsø meteorological station were used to interpret the major processes contributing to variations in particle concentration in the snow. Other factors that can affect snowmelt include relative humidity, vapor pressure, and snowpack conditions (such as density) (Skiles et., 2012).

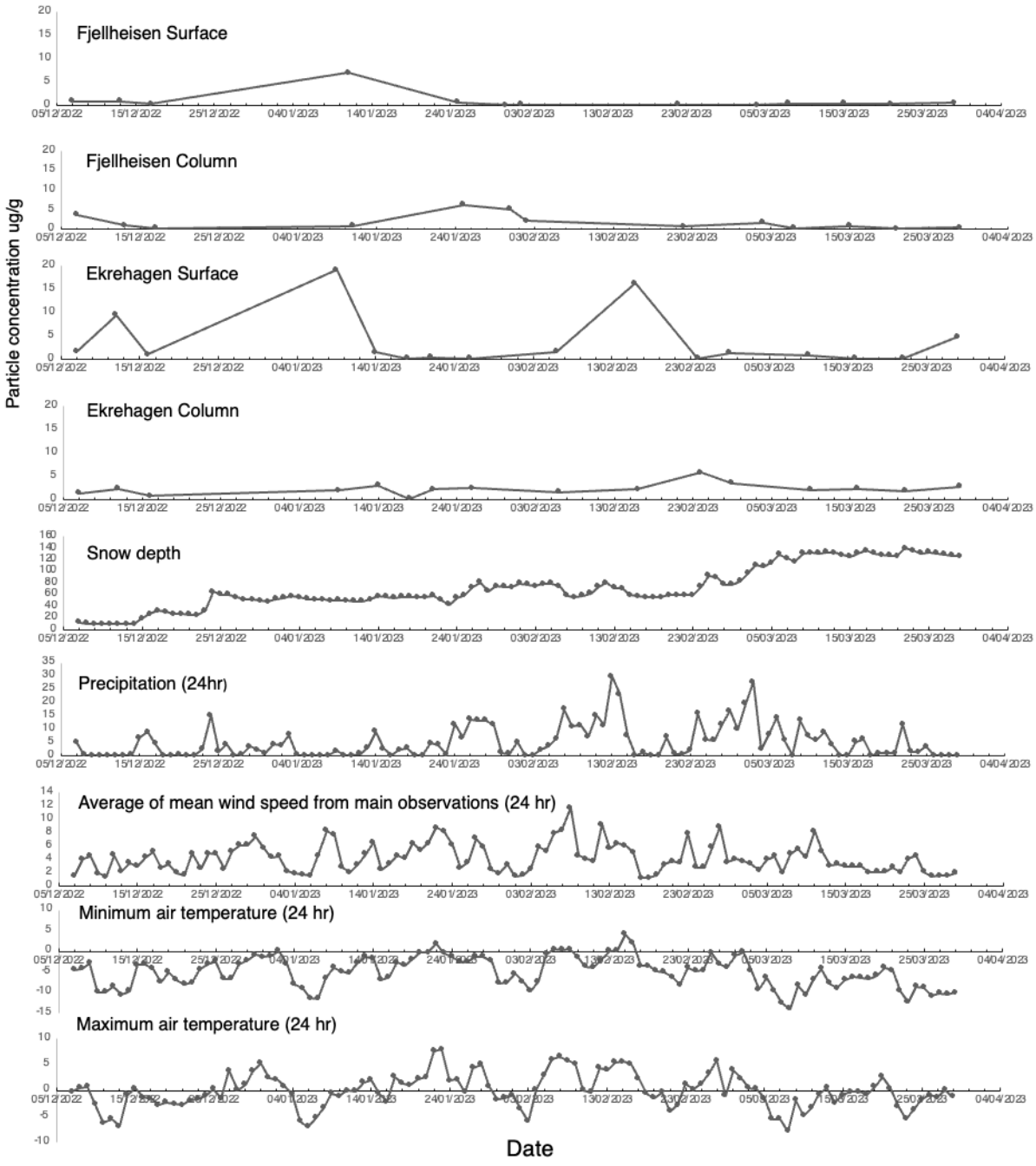

Figure 21. Meteorological data from the Norwegian Centre for Climate Services and particle concentration (without LOM) plotted against date.

The highest particle concentration sampled at Fjellheisen occurred in January, while the rest of the season was characterized by lower particle concentration. Towards the start of the winter season, the particle concentration in Fjellheisen surface and column were similar, with slightly higher particle concentration in Fjellheisen column. Fjellheisen column particle concentration decreased between December 7, 2022, to December 17, 2022, and remained low on December

17, 2022, and January 11, 2023 (no other sampling occurred between these two dates). The surface particle concentration increased on January 11, 2023, to the highest surface concentration in the record. Meteorological data indicates that the surface particle concentration increase may have occurred because of a long period of little additional snow accumulation that preceded sampling on January 11, 2023. Additionally, the wind events on January 8 and 9, 2023 that occurred prior to sampling also suggests both dust and large organic matter observed on the filters (Figure 16) could have been transported from local sources and deposited on the snow. The increase in temperature between January 6 and January 11, 2023, from the meteorological data suggest that during this period, the snow melted which also explains the enhancement of particle concentration at the surface layer on January 11, 2023. During this warming period a small decrease in the snow depth is also observed in the meteorological data. However, a temperature above 0 °C in the Tromsø data does not necessarily mean it was above freezing at Fjellheisen, since it is colder at higher elevations. This is discussed later in section 4.3. Earlier studies have shown that particle concentration increases at the snow surface as a result of mechanical trapping, during melt or sublimation, with vigorous melt conditions flushing particles deeper into the snowpack (Xu et al., 2012; Conway et al., 1996). The highest particle concentration in the column layer was on January 25, 2023, followed by January 31, 2023, and then February 2, 2023, with particle concentrations of 6.33 µg/g, 5.12 µg/g and 2.19 µg/g, respectively. The meteorological data shows an increase in precipitation and snow between January 23 to January 27, 2023, indicating new snow accumulation that coincides with a decrease in the surface particle concentration. The particle concentration in the column layer increased because the high concentration layer that was previously at the surface is now sampled in the column after new deposition of snow. The particle concentration in the column is lower than when that layer was at the surface because of differences in sampling resolution. When this high concentration layer which was previously at the surface was sampled, it was sampled as a concentrated layer; when buried below and sampled in the column, it was sampled with a much larger volume of snow, which caused the measured particle concentration to appear lower in the column than when it was at the surface.

4.2 Variation in particle concentration between Ekrehagen surface and column

Similar to Fjellheisen, the particle concentration in the Ekrehagen column layer tends to be higher than the surface layer (Table 8). For the whole season, the mean particle concentration is higher in the column layer than the surface layer (2.14 μg/g and 1.07 μg/g respectively).

The highest particle concentrations sampled at Ekrehagen occurred in January followed by in February, while the rest of the season was characterized by lower particle concentration. On December 12, 2022, the surface layer had higher particle concentration relative to the column layer, which may be due to high winds between December 10, 2022, to December 12, 2022, that deposited particles onto the snowpack. At Ekrehagen, there are high particle concentrations in both the surface and column layer towards the start of the winter season. There are two events on January 9, 2023, and February 16, 2023, when high particle concentrations occurred in the surface layer at Ekrehagen. The event of January 9 corresponds to the same surface high particle concentration event that was observed at Fjellheisen following a long period of little additional accumulation that preceded sampling on January 9, 2023. The high particle concentration event on February 16, 2023, is associated with a dry period, although, the wind event that happened on February 8, 2023, might have also contributed to deposition of particles onto the snow. Meteorological data shows snow depth decreased before sampling on February 16, 2023, which indicates that the high particle concentration at the surface layer was due to a dry period (Davidson et al., 1985; Skiles et al., 2018), and the sample is considered "aged snow". A few days period without precipitation, combined with above zero temperature at this time suggests there may have been some melt. Surface darkening brought on by dirty snow will hasten the ageing of the snow, which further reduces snow albedo and speeds up snowpack melt (Flanner et al., 2007).

The particle concentrations in the surface layer were low on February 24, February 28, March 10, March 16 and in March 2023 as the snow depth increases indicating that fresh snow with low particle concentrations continued to be deposited at the surface. The surface layer which was previous at the top of the snowpack was buried below, hence diluting the particle concentration in the whole snowpack (newly accumulated snowfall and the previous layer with high concentration at the surface). This explains why the sample collected on February 24, 2023, had a high particle concentration at the column layer relative to the surface layer. The particle concentration in the column layer gradually decreases from February 24 to February 28 to March 10, 2023, as fresh snow continues to fall, and a new layer continues to build on top

of the snow. This explain that the high particle concentration layer which was previous at the surface is now sampled as column also continues to get deeply buried below as the snow depth increases, hence diluting the particle concentration and reducing the particle concentration in the column layer when the column layer is sampled with a much larger volume of snow.

Towards the end of March when snow started to melt, the snow depth gradually starts to decrease. The particle concentration in the surface layer on March 29, 2023, was higher than on March 22, 2023, when it was still snowing, indicating that the snow melt was responsible for enhancement of particle concentration at the surface layer. This is consistent with the findings of Doherty et al. (2010) that surface concentration increases as the snow melts. In this study, sampling was stopped on March 29, 2023, however earlier studies have demonstrated that particle concentration increases in the surface layer during the spring, possibly due to a spring peak in the atmospheric transport of pollutants to the Arctic (e.g., Stohl, 2006; Quinn et al., 2007) which causes enhanced deposition; the melting of the surface snow that leaves insoluble particles at the surface; or to climatological precipitation minimum in spring that keeps the same surface exposed to dry deposition for long time (Meyer and Wania, 2008; Doherty et al., 2013). In the column layer, the particle concentration on the last day of sampling (March 29, 2023) was high relative to the particle concentration on March 22, 2023 as the snow depth decreases, which indicates that the column layer was sampled with lesser volume of snow as there was no new snowfall to increase dilution of particle concentration across the whole snow column, hence the difference in the particle concentration between sample collected on March 29, 2023 and March, 22, 2023.

4.3. Comparison of particle concentration between Fjellheisen and Ekrehagen

Throughout the whole of the season, the mean particle concentrations are higher at Ekrehagen than at Fjellheisen, and the highest maximum particle concentration in the data set is at 19.12 µg/g from an Ekrehagen surface sample on February 16, 2023 (Table 8). The same factors (wind, lower snow accumulation, and rise in temperature) contributed to the enhancement of particle concentration at the surface layer in Ekrehagen surface and Fjellheisen surface during the month of January. There are two possible explanations for the higher particle concentration at Ekrehagen in comparison to Fjellheisen, both which are associated to elevation gradient. There were several rain events at Ekrehagen in February during the time of sample collection. The snow depth from the meteorological data also indicates that there was melt and precipitation which was in form of rain in February. However, due to the elevation gradient,

between Fjellheisen (420 m above sea level) and Ekrehagen (70 m, above sea level), the snow melt that occurred at Ekrehagen mostly likely did not happen at Fjellheisen due to the elevation gradient and atmospheric lapse rate, in which the temperature of the atmosphere decreases with increasing altitude. Fjellheisen being 350 m higher in elevation than Ekrehagen. During this period, the temperature from the meteorological data in Tromsø shows that the temperature was 5.6 °C, meaning that the temperature at Fjellheisen would have been 2.1 °C for dry air and 1.75 °C for wet air, since temperature reduces with an increase in elevation by 1 °C per 100 m in dry air and 1°C per 200 m for saturated air. A temperature above 0 °C in the Tromsø data does not necessarily mean it was above freezing at Fjellheisen, since it is colder at higher elevations. This suggest that the snow melt that occurred at Ekrehagen mostly likely did not happen at Fjellheisen because of the elevation gradient. Additionally, higher elevation at Fjellheisen could have resulted in snow while it was raining at Ekrehagen. The lower snow accumulation at Ekrehagen caused the particles to be slightly more concentrated in the snowpack, and there possibly was higher particle deposition from local sources. Dumka et al. (2011) has demonstrated that particle concentration will decrease with an increase in altitude which also explains why the particle concentration at Ekrehagen is higher than at Fjellheisen.

4.4 Effect of meteorological factors on snow particle concentration

Wind, precipitation, temperature, and snow depth are the major meteorological factors affecting the concentration of particles in snow. The wind plays the major role in enhancing particle concentration at both sites (Fjellheisen and Ekrehagen). The majority of the time when particle concentrations are high on the filters follows a wind event, which suggests that the wind is responsible for transporting particles and large organic matter either by transporting the particle along with the snow or deposition of the particles from local sources on to the snow cover. Temperature also plays an important role in enhancing particle concentration. A small rise in temperature can cause the snow to melt if temperatures are near freezing, which reduces snow depth and enhances particle concentration at the surface layer. However, if the temperature is well below freezing, a small increase in temperature will not do this. A typical example is the sample collected at Ekrehagen on February 16, 2023, when the temperature was above 0 °C; the snow had melted and caused mechanical trapping of particles at the surface layer. Precipitation also affects particle concentration on the snow; the particle concentration for Ekrehagen and Fjellheisen surface layer was low when it was continuously snowing in mid-January to early-February. During this period of continuous snowfall, the snow depth increased, forming a new snow layer on top of the previous higher particle concentration layer and burying

the high particle concentration layer below. Eventually the surface layer with high concentration gets buried below. Lower concentrations of BC should typically be found in the snowpack at places with higher precipitation for a given concentration of BC in the atmosphere. Even if wet deposition predominates, the effect of more precipitation diluting the BC in the snow should still be there. This effect should be especially strong if dry deposition predominates (Forsström et al., 2013).

4.5 Relative contribution of black carbon and dust to snow albedo reductions

Past studies in Tromsø were focused exclusively on BC, but the role of dust in albedo reduction is also important. The SNICAR model was used to evaluate the contribution of BC and dust to albedo reduction (Flanner et al., 2007). SNICAR was run for three distinct scenarios (only BC, only dust, and BC + dust) (Figures 22, 23, 24 and 25). BC concentrations from previous studies in Tromsø from Pedersen et al. (2015), Doherty et al. (2013), and Forsström et al. (2013) were used assuming that the measured concentrations reflect BC and particle concentration that resided on the surface in the past (Table 4). In this study, the modeled albedo was calculated based on the dust concentration for winter. Because some of the measured particle mass may be organic and not mineral dust, 50% and 75% dust scenarios (meaning 50% and 75% of the measured particle mass) were run to account for the plausible range of particle concentration that may be mineral dust (e.g., not organic). There is currently no data for dust concentration that is from the same condition (late season melt) as when BC concentration was 75 ng/g and 1542 ng/g (Figure 22). The high concentration of BC at 75 ng/g and 1542 ng/g from previous studies is representative of late spring conditions when more particles would be concentrated at the surface layer and solar insolation would be at the highest. The concentration of BC in late spring compared to the BC concentration in winter (1542 µg/g and 3 ng/g respectively) shows that the BC concentration increased by 514x from winter to late spring. Based on how much BC increased during the melt season can be used to estimate the increase in particle concentration in late spring. Assuming the concentration of particle increased by 450x and 250x in late spring from its median concentration in winter (3.62 µg/g), the spring dust particle concentration would be 1629 µg/g and 905 µg/g respectively (Table 9). The SNICAR model runs of spectral snow albedo assumes that snow density, snow thickness, snow grain effective radius and snow grain shape are the same for all scenarios since investigating differences in albedo reductions for different LAP scenarios is the focus of this study. However, in actuality

these parameters would change over the course of the snow season. Figure 23, 24 and 25 shows that the higher the particle concentration in the snowpack, the lower the broadband snow albedo (Skiles et al., 2018).

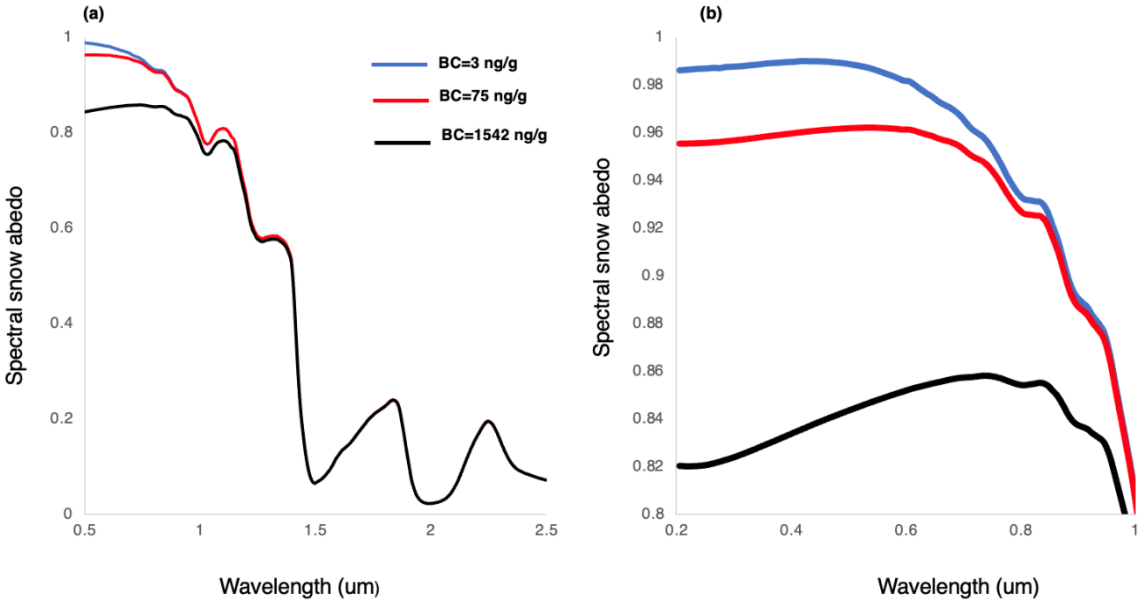

Figure 22. SNICAR modeled spectral snow albedo based on BC mean, median and maximum concentrations using BC concentration from previous studies in Tromsø (a) SNICAR modeled spectral snow albedo between 0 to 1 range between the wavelength of 0.5 µm to 2.5 µm (b) SNICAR modeled spectra snow albedo between 0.9 to 1 ranging between a wavelength of 0.2 µm to 1.0 µm.

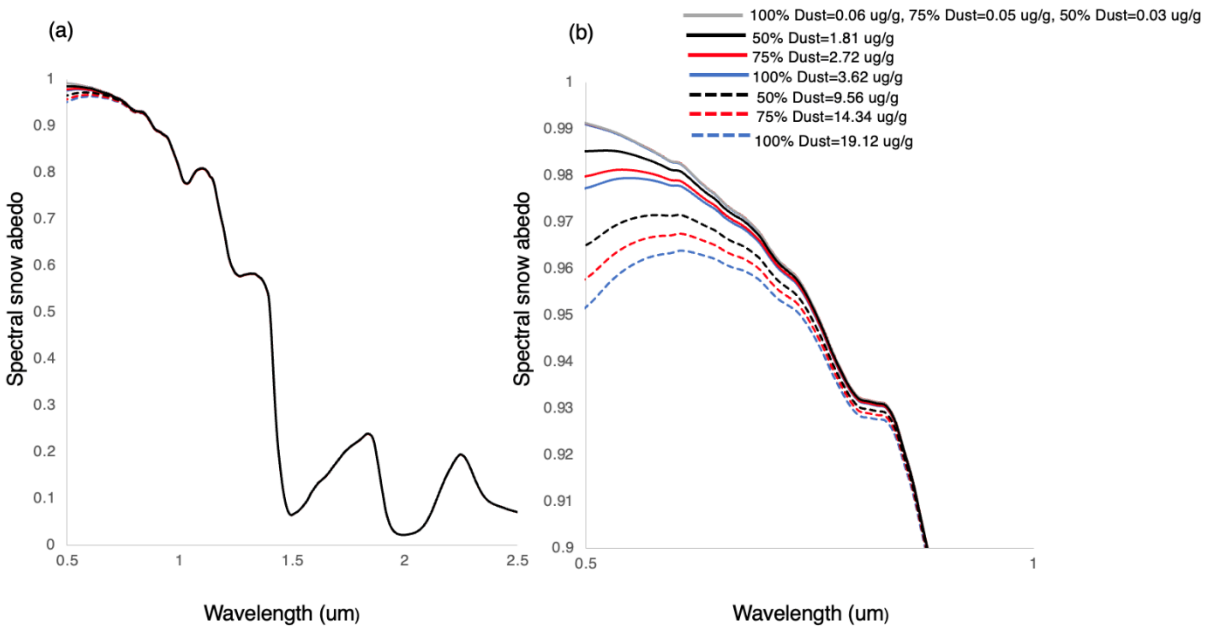

Figure 23. SNICAR modeled snow spectral albedo for dust mean, median and maximum concentrations (a) SNICAR modeled snow spectral albedo between 0 to 1 at 0.5 µm to 2.5 µm wavelength (b) SNICAR modeled snow spectral albedo between 0.9 to 1 at a wavelength 0.5 µm to 1.0 µm.

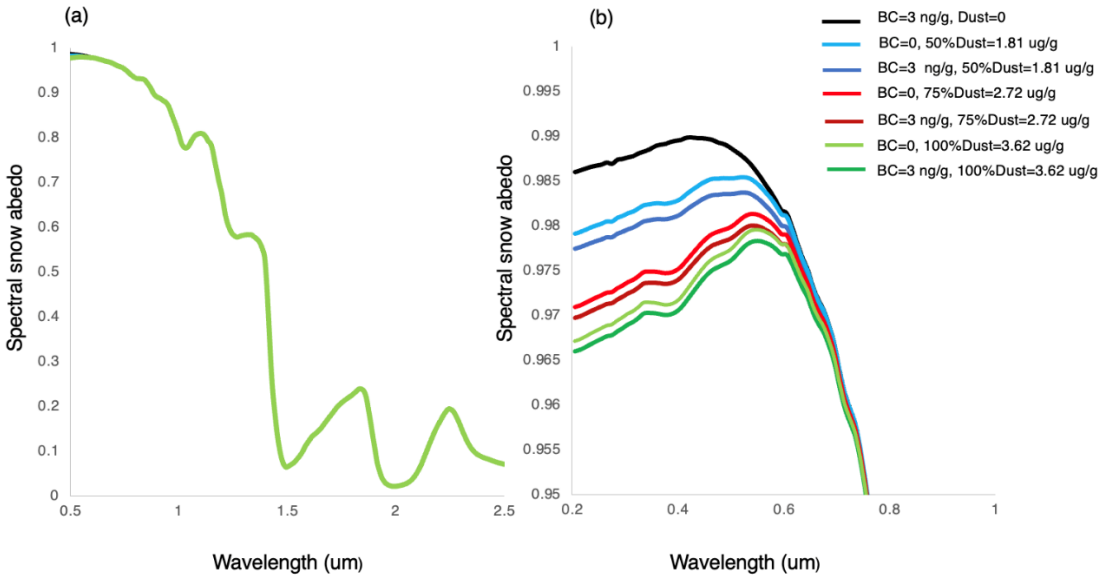

Figure 24. SNICAR modeled spectral snow albedo for minimum BC and dust assuming measured concentrations reflect BC and particle concentration that resided on the snow surface in the past. (a) SNICAR modeled spectral albedo between 0 to 1 at wavelength of 0.5 µm to 2.5 µm (b) SNICAR modeled spectra albedo between 0.95 to 1 at wavelength 0.2 µm to 1 µm.

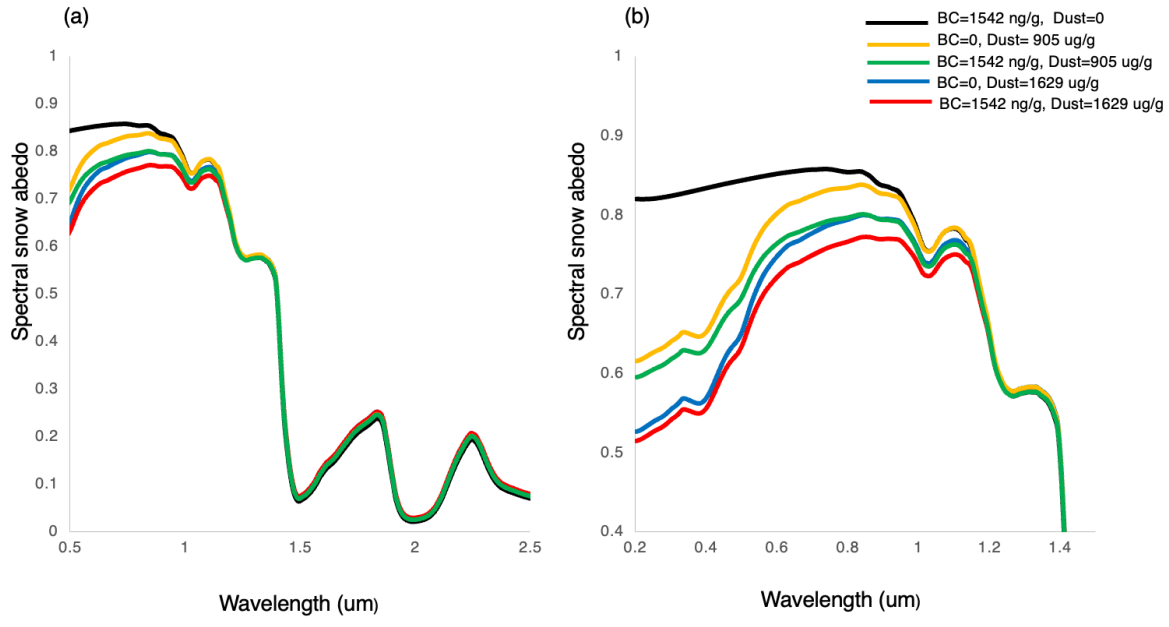

Figure 25. SNICAR modeled spectral snow albedo for BC and dust concentrations that are representative of the spring melt season. (a) SNICAR modeled spectral albedo between 0 to 1 at wavelength of 0.5 µm to 2.5 µm (b) SNICAR modeled spectral albedo between 0.4 to 1 at wavelength of 0.2 µm to 1.5 µm.

Scenario name	Particle type	Broadband snow albedo
BC=3, no dust	BC	0.908
BC=75, no dust	BC	0.892
BC=1542, no dust	BC	0.803
100%Dust=0.06 no BC	Dust	0.909
100%Dust=3.62, no BC	Dust	0.902
100%Dust=19.12, no BC	Dust	0.888
75%Dust=0.05, no BC	Dust	0.909
75%Dust=2.72, no BC	Dust	0.903
75%Dust=14.34, no BC	Dust	0.891
50%Dust=0.03, no BC	Dust	0.909
50%Dust=1.81, no BC	Dust	0.906
50%Dust=9.56, no BC	Dust	0.895
BC=3, 50%dust=1.81	BC + Dust	0.905
BC=3, 75% dust=2.72	BC + Dust	0.902
BC=3, 100%dust=3.62	BC + Dust	0.901
BC=1542, dust=1629	BC + Dust	0.663
BC=1542, dust=905	BC + Dust	0.706
Dust=1629	Dust	0.684
Dust=905	Dust	0.735

Table 9. SNICAR model for different scenarios of BC (ng/g), dust (μg/g) and BC + dust.

The SNICAR modeled spectral snow albedo (Figure 22, 23, 24 represents low particle concentrations typical of the winter snowpack. Figure 22 shows SNICAR modeled spectral snow albedo for BC mean, median and maximum concentration and Figure 23 shows SNICAR modeled spectral snow albedo for mean, median and maximum concentration of dust assuming that dust and BC are mixed in the snowpack. The broadband albedo decreases with increase in concentration of BC and dust (Table 9), and the broadband albedo decreases with an increase in the proportion of the particle concentration that is assumed to be dust (from 50% to 75% and 100%, Table 9). This indicates that broadband snow albedo decreases with higher particle concentration in the snowpack (Skiles et al., 2018), however the broadband albedo reductions during winter are very small relative to clean snow.

To compare the relative contribution of BC and dust to snow albedo reduction in winter, SNICAR model was run for BC and dust for minimum concentration in winter (Figure 24) (Table 9). The SNICAR modeled spectral snow albedo (Figure 24) shows that BC with a concentration of 3 ng/g lowers broadband snow albedo by 0.092 relative to clean snow. In contrast, dust with a concentration of 1.81 µg/g, 2.72 µg/g, and 3.62 µg/g (based on the 50%, 75% and 100% dust scenarios) lowers broadband albedo by 0.094, 0.097, and 0.098, respectively, relative to clean snow. Importantly, these results show that the albedo reductions only due to dust are greater than the albedo reduction from only BC. Even a dust concentration of 1.81 µg/g lowers broadband albedo more than BC with a concentration of 3 ng/g.

To compare the relative contribution of BC and dust to snow albedo reduction both in winter and spring, the SNICAR model was run for different scenarios assuming both BC and dust are mixed in the snowpack in winter (Figure 24) and in late spring (Figure 25). Assuming in winter, BC and dust are mixed in the snowpack with BC having a concentration of 3 ng/g and 50% of the particle concentration is dust with a concentration of 1.81 µg/g, the modeled broadband reduces by 0.003 relative to if BC was only in the snowpack, If BC is 3 ng/g and 75% of the particle is dust with a concentration of 2.72 µg/g, the modeled broadband snow albedo is 0.902, indicating that broadband albedo reduced by 0.006 relative to if BC only was in the snowpack. For the third scenario in winter, assuming all the particle is mineral dust (i.e. 100% dust) with a concentration of 3.62 µg/g and BC with a concentration of 3 ng/g, the modeled broadband snow albedo is 0.901, indicating that the inclusion of dust mixed in the snowpack with BC lowers broadband albedo by 0.007 relative to if BC only was in the snowpack (Table 10). This indicates that the inclusion of dust with BC in the snowpack would cause the broadband albedo to be lower than if BC was the only LAP in the snowpack. This is consistent with the findings

of Kaspari et al. (2011) that albedo reductions from BC will be less in the presence of other light absorbing particles because the other particles absorb some of the solar radiation that the BC would receive in the absence of other particles. Prior research has demonstrated that non-BC components account for up to 25–50% of the particulate light absorption in Arctic snow (Bond et al., 2013).

For the SNICAR modeled spectral snow albedo for late spring, two assumptions on how particle concentration can increase in late spring were made, and five different scenarios (Figure 24) were modeled for spectral broadband snow. If only BC was in the snowpack with a concentration of 1542 ng/g, the modeled broadband snow albedo is 0.803, and 20% lower relative to clean snow. If only dust was in the snowpack with a concentration of 1629 µg/g, and 905 µg/g, the modeled broadband albedo is 0.684 and 0.735, respectively, representing a 32% and 27% reduction in albedo relative to clean snow. This shows that albedo reduction due to dust are higher than BC.

If BC with a concentration of 1542 ng/g and dust with a concentration of 1629 µg/g are mixed in the snowpack, the broadband model albedo is 0.663. This shows that dust with BC in snowpack will lower the snow albedo by 34% relative to clean and 17% more than if only BC was in the snowpack, and 3% more than the only dust scenario. For the second scenario assuming that dust particle increased by 250x from its median winter concentration, if BC with a concentration of 1542 ng/g and dust with a concentration of 905 µg/g are mixed in the snowpack, the broadband albedo is 0.706. This indicates that dust with BC in the snowpack will lower snow albedo by 30% relative to clean snow, 12% more than if only BC was in the snowpack, and 4% more than only dust. These results shows that dust will be a larger contributor of snow albedo reduction in late spring.

In winter, the SNICAR modeled snow albedo for 100% dust with a concentration of 3.62 µg/g and BC concentration of 3 ng/g is 0.901, while the broadband snow albedo for late spring is 0.663 and 0.706 if particle concentration increases by 450x and 250x respectively. This represents a 26% decrease in broadband albedo for 450x increase and 22% decrease for 250x increase in particle concentration for the spring melt period relative to winter, meaning that 26% more of the incoming solar energy is being absorbed by the snowpack in spring relative to winter and contributing to melt. The results from the SNICAR modeled run indicates that dust will dominate albedo reduction both in winter and late spring but will contribute more to albedo reduction in late spring than in winter. This is a large change in the surface energy

balance. The SNICAR model runs in this study only considered changes in BC and dust concentration and did not account for changes in snow grain size and density, nor brown carbon, all of which would result in a further spring albedo reduction.

The most prevalent atmospheric aerosol by mass is dust, which is produced in arid and semi-arid environments (Andreae, 1995). Despite being a naturally occurring aerosol by mass (Tegen & Schepanski, 2018), dust is a greater driver in reducing snow albedo. Previous research has revealed that atmospheric dust has nearly doubled since the turn of the 20th century (Mahowald et al., 2010). Most likely as a result of human land use patterns and drought brought on by climate change. Dust is more likely to be found in snow cover that is downwind from large arid and semi-arid regions that have been disturbed (Franzén et al., 1994; Painter et al., 2007; Thompson et al., 2000; Di Mauro et al., 2015). Given the clear anthropogenic origin of the rise in BC and the fact that dust is much less absorptive than BC, dust in snow has received less attention in terms of its effects on the climate. However, recent research has demonstrated that, in the presence of sufficiently high concentration of dust, radiative forcing by dust can dominate albedo reductions in snow (Skiles & Painter, 2018; Sterle et al., 2013; Kaspari et al., 2014). Therefore, it is important to include dust in analyses of dust in albedo reductions. In addition to BC and dust, other light absorbing particles that can lower albedo include light absorbing carbon (coloured organics) from biomass burning, humic-like materials, snow algae, and bacteria (Andreae and Gelencser, 2006; Takeuchi, 2002; Painter et al., 2007).

4.6 Snow reflectance at Ekrehagen and Fjellheisen

The snow reflectance at Ekrehagen (112% at 400-700 nm) was higher than that of Fjellheisen (104% at 400-700 nm) for the snow reflectance measurement taken on March 29, 2023 (Figure 18). Although, snow reflectance should not be greater than 100%, the higher values were due to the low angle of sun and the snow crystals reflecting light in numerous directions resulting in a higher measured reflectance than the Spectralon panel that was used to calibrate the instrument (the white square panel) (Figure19).

It is expected that the particle concentration in surface snow is higher at Fjellheisen than at Ekrehagen since the snow reflectance at Ekrehagen is higher than at Fjellheisen for the measurement taken on March 29, 2023. However, the snow surface particle concentration at Ekrehagen was higher than at Fjellheisen (4.82 μg/g and 0.54 μg/g respectively) (Table 7). Figure 19 visually shows the difference between the surface snow at Ekrehagen and Fjellheisen.

The white and black reflectance standards at Ekrehagen surface (Figure 20) sunk in the snow, whereas the white and black standards at Fjellheisen didn't sink but stayed at the surface indicating that the surface snow at Ekrehagen was lower density relative to the surface snow at Fjellheisen.

The SNICAR model was used to model different runs based on different snow density and grain size to see if these parameters could account for the difference observed in snow reflectance (Table 10).

Site	Scenario	Particle concentration (µg/g)	Density (kg/m^3)	Snow grain radius (µm)	Broadband albedo
Ekrehagen	1	4.82	200	100	0.900
Fjellheisen	2	0.54	200	100	0.908
Ekrehagen	3	4.82	200	50	0.921
Fjellheisen	4	0.54	200	50	0.927
Ekrehagen	5	4.82	100	100	0.901
Fjellheisen	6	0.54	100	100	0.908
Ekrehagen	7	4.82	100	50	0.921
Fjellheisen	8	0.54	100	50	0.925

Table 10. SNICAR modeled spectral snow albedo based different snow density and grain size for Ekrehagen and Fjellheisen surface particle concentration on March 29, 2023.

For the SNICAR model run the particle concentration for both sites (Ekrehagen and Fjellheisen) on March 29, 2023, were kept constant, 4.82 μg/g and 0.54 μg/g, respectively for modeling all different scenarios. The SNICAR modeled spectral snow albedo (Table 10) shows the broadband albedo for all eight scenarios using different densities and snow grain sizes.

Scenario 1 to 4 demonstrate that smaller snow grain sizes will have a higher broadband snow albedo. A reduction in density also results in a slightly higher broadband albedo (scenario 4 to 8). The SNICAR modeled broadband spectral albedo for scenario 2, with particle concentration of 0.54 μg/g, 200 kg/m^3 density and 100 μm results in a broadband albedo of 0.908. Scenario 7, with particle concentration of 4.82 μg/g, 100 kg/m^3 density and 50 μm results in a broadband albedo of 0.921. The different in snow density and grain size indicates why Ekrehagen can have a higher snow reflectance than Fjellheisen despite having higher particle concentration. The lower density of surface snow at Ekrehagen relative to Fjellheisen surface snow suggests that the snow grain size in the snowpack at Ekrehagen are smaller than that at Fjellheisen surface which is why the snow crystals at Ekrehagen surface are reflecting more light than at Fjellheisen surface snow. Snow albedo will decrease in the longer wavelength as snow grain size increases (Skiles et al., 2018). Snow grain size are important parameters and should be considered when modeling.

CHAPTER 5. SUMMARY, CONCLUSION AND RECOMMENDATIONS

5.1 Summary and Conclusion

Snow samples were collected in Tromsø (Fjellheisen and Ekrehagen), Norway during the winter season from December 2022 to March 2023, both from surface snow and vertical profiles through the snow column. The samples were analyzed for particle concentration using gravimetric filtration, which provides a proxy of dust deposition. To understand variability in particle concentration between the surface layer and column layer from both sites over time, meteorological data including snow depth, precipitation, average mean wind speed, and minimum and maximum temperature (24 hr) from the Norwegian Centre for Climate Services was used to interpret the major process contributing to particle concentration in the Norwegian Arctic snow. Snow reflectance was measured at Fjellheisen and Ekrehagen using a spectroradiometer to estimate the variation in snow reflectance from both sites. The SNICAR model was used to evaluate the relative contribution of BC and dust to albedo reductions (Flanner et al., 2007), and was run assuming that that the measured particle concentrations reflect BC and particle concentration that resided on the surface in the past. However, for the purpose of this study, there is no equivalent measurement of particles from this same time period in the melt season, but based on how much BC increased during the melt season can be used to estimate the increase in particle concentration in late spring. The concentration of BC in late spring compared to BC concentration in winter (1542 ng/g and 3 ng/g, respectively) shows that the BC concentration increased by 514x from winter to late spring. If particle concentration also increases by 450x or at least 250x from its median concentration in winter, the particle concertation will be 1629 µg/g and 905 µg/g respectively in late spring. The findings from this study show that:

- Snow melt during warm periods, long dry periods of little additional accumulation of snowfall, and wind all enhance particle concentration in the surface layer of the snowpack. This is consistent with the findings of Doherty et al. (2013).
- Additional accumulation of fresh snowfall with low gravimetric particle concentration leads to low particle concentration in the surface layer of the snowpack.
- Accumulation of new fresh snowfall on a high particle concentration layer will lead to formation of a new layer at the surface, hence burying the high concentration layer below. When this high particle concentration surface layer is buried by fresh snowfall, the measured particle concentration in the column will increase because the high particle

layer that previously resided at the surface is now being sampled as vertical column. Measured column particle concentrations were lower than surface particle concentrations because the high concentration layers are diluted with a large volume of snow in the column.

- The higher the concentration of LAPs (BC and/or dust) in snow, the lower the broadband snow albedo.
- Low density snow has a higher albedo than higher density snow because lower density snow has smaller grain size, which can reflect more light.
- Snow particle concentrations are higher at Ekrehagen (70 m a.s.l.) than Fjellheisen (420 m a.s.l.) due to the 350 m elevation difference of the two sites. Ekrehagen has a higher occurrence of melt and rain, both of which increase particle concentrations, while Fjellheisen receives more snow and has a lower occurrence of times when particle concentrations are high on the surface of the snowpack. This has implications under a changing climate. As climate warms, more areas are more likely to get more rain and to have higher particle concentration surfaces, resulting in lower albedo, greater energy absorption, more melt of the snowpack and more energy kept in the Earth System.
- The SNICAR modeled spectral snow albedo indicates that dust is a greater driver of albedo reduction than BC. However, the combination of BC and dust results in a further lower albedo reduction, but dust is the LAP that is the strongest driver of albedo reductions in the snow.
- The results from the SNICAR modeled snow albedo indicates that dust dominates albedo reduction both in winter and late spring, with larger albedo reductions in late spring than in winter. For the minimum and maximum concentration, the modeled spectral snow albedo shows that broadband albedo in winter is 0.901, and the broadband spectral albedo in spring is 0.663 and 0.706 if dust increases by 450x and 250x respectively from its minimum concentration in winter. This indicates that 22% to 26% more of the incoming solar energy is being absorbed by the snowpack in spring relative to winter and contributing to melt (assuming dust increases by 250x and 450x respectively). This is a large change in the surface energy balance. However, the SNICAR model runs in this study only considered changes in BC and dust concentration and did not account for changes in snow grain size and density, nor brown carbon, all of which would result in a further spring albedo reduction.

- Even though dust is a naturally occurring aerosol, it is a greater driver in snow albedo reductions than BC. Previous studies have demonstrated that atmospheric dust has doubled since the turn of 20th century, which is most likely due to anthropogenic effect and drought brought on by climate change. However, dust has received less attention in terms of its effect on the climate. This research has demonstrated that in the presence of high concentration of dust (in spring), radiative forcing from dust can dominate albedo reduction in snow. Therefore, it is important to include dust in the analyses of LAP albedo reductions in snow.

5.2 Recommendations for future research

- Measure snow density of the snowpack.
- Sample the snowpack at higher vertical resolution. Because high sample volumes were required for the gravimetric particle analysis, the study was designed to collect bulk samples of the surface and column. If samples were collected at higher vertical resolution, the presence of high particle layers in the snowpack could have been better traced.
- Determine particle size distribution, which is useful for albedo modeling and to evaluate how the particles were transported (i.e., local vs. long range transport).
- Determine the proportion of particles that are organic vs mineral dust to evaluate which are likely important drivers of albedo reductions and snow melt.
- Future studies should focus on sampling BC concentration and dust concentration together at the same period to determine the relative contribution of BC and dust to albedo reduction for SNICAR modeling. Although samples were collected for BC analysis for this study, the results were not available in time to be incorporated in this thesis.
- Calculate the proportionate contributions of each to albedo reductions by geochemically dividing LAP into BC, dust, and organics**.**
- The sampling period should be extended (i.e., samples should be collected from early winter until the snow completely disappears in late spring-summer).

References

Andreae, M. O., & Gelencsér, A. (2006, July 28). Black carbon or brown carbon? The nature of light-absorbing carbonaceous aerosols. Atmospheric Chemistry and Physics, 6(10), 3131–3148. https://doi.org/10.5194/acp-6-3131-2006.

Andreae, M.O. (1995) Climatic Effects of Changing Atmospheric Aerosol Levels. In: Henderson-Sellers, A., Ed., World Survey of Climatology, Vol. 16, Future Climates of the World, Elsevier, Amsterdam, 341-392.

Aoki, T., Motoyoshi, H., Kodama, Y., Yasunari, T. J., Sugiura, K., & Kobayashi, H. (2006). Atmospheric Aerosol Deposition on Snow Surfaces and Its Effect on Albedo. SOLA, 2(0), 13–16. https://doi.org/10.2151/sola.2006-004.

Bian, H., Colarco, P. R., Chin, M., Chen, G., Rodriguez, J. M., Liang, Q., Blake, D., Chu, D. A., da Silva, A., Darmenov, A. S., Diskin, G., Fuelberg, H. E., Huey, G., Kondo, Y., Nielsen, J. E., Pan, X., & Wisthaler, A. (2013, May 7). Source attributions of pollution to the Western Arctic during the NASA ARCTAS field campaign. Atmospheric Chemistry and Physics, 13(9), 4707–4721. https://doi.org/10.5194/acp-13-4707-2013.

Bintanja, R., Graversen, R. G., & Hazeleger, W. (2011, October 16). Arctic winter warming amplified by the thermal inversion and consequent low infrared cooling to space. Nature Geoscience, 4(11), 758–761. https://doi.org/10.1038/ngeo1285.

Birch, M. E. (2003), Elemental carbon (diesel exhaust): Method 5040, in NIOSH Manual of Analytical Methods, National Institute of Occupational Safety and Health, pp. 1–5, National Institute of Occupational Safety and Health, Cincinnati, Ohio.

Bond, T. C. (2004). A technology-based global inventory of black and organic carbon emissions from combustion. Journal of Geophysical Research, 109(D14). https://doi.org/10.1029/2003jd003697.

Bond, T. C., & Bergstrom, R. W. (2006, January 1). Light Absorption by Carbonaceous Particles: An Investigative Review. Aerosol Science and Technology, 40(1), 27–67. https://doi.org/10.1080/02786820500421521.

Bond, T. C., Doherty, S. J., Fahey, D. W., Forster, P. M., Berntsen, T., DeAngelo, B. J., Flanner, M. G., Ghan, S., Kärcher, B., Koch, D., Kinne, S., Kondo, Y., Quinn, P. K., Sarofim, M. C., Schultz, M. G., Schulz, M., Venkataraman, C., Zhang, H., Zhang, S., . . . Zender, C. S. (2013, June 6). Bounding the role of black carbon in the climate system: A scientific assessment. Journal of Geophysical Research: Atmospheres, 118(11), 5380–5552. https://doi.org/10.1002/jgrd.50171.

Bourgeois, Q., & Bey, I. (2011, April 27). Pollution transport efficiency toward the Arctic: Sensitivity to aerosol scavenging and source regions. Journal of Geophysical Research, 116(D8). https://doi.org/10.1029/2010jd015096.

Box, J. E. (2013). Greenland Ice Sheet Mass Balance Reconstruction. Part II: Surface Mass Balance (1840–2010)*. Journal of Climate, 26(18), 6974–6989. https://doi.org/10.1175/jcli-d-12-00518.1.

Box, J. E., Fettweis, X., Stroeve, J., Tedesco, M., Hall, D., & Steffen, K. (2012). Greenland ice sheet albedo feedback: thermodynamics and atmospheric drivers. The Cryosphere, 6(4), 821–839. https://doi.org/10.5194/tc-6-821-2012.

Box, J. E., Van As, D., & Steffen, K. (2017). Greenland, Canadian and Icelandic land-ice albedo grids (2000–2016). Geological Survey of Denmark and Greenland Bulletin, 38, 53–56. https://doi.org/10.34194/geusb.v38.4414.

Boy, M., Thomson, E. S., Acosta Navarro, J. C., Arnalds, O., Batchvarova, E., Bäck, J., Berninger, F., Bilde, M., Brasseur, Z., Dagsson-Waldhauserova, P., Castarède, D., Dalirian, M., de Leeuw, G., Dragosics, M., Duplissy, E. M., Duplissy, J., Ekman, A. M. L., Fang, K., Gallet, J. C., . . . Kulmala, M. (2019, February 14). Interactions between the atmosphere, cryosphere, and ecosystems at northern high latitudes. Atmospheric Chemistry and Physics, 19(3), 2015–2061. https://doi.org/10.5194/acp-19-2015-2019.

Budyko, M. I. (1969, January 1). The effect of solar radiation variations on the climate of the Earth. Tellus A: Dynamic Meteorology and Oceanography, 21(5), 611. https://doi.org/10.3402/tellusa.v21i5.10109.

Cavalli, F., Viana, M., Yttri, K. E., Genberg, J., & Putaud, J. (2010). Toward a standardised thermal-optical protocol for measuring atmospheric organic and elemental carbon: the EUSAAR protocol. Atmospheric Measurement Techniques, 3(1), 79–89. https://doi.org/10.5194/amt-3-79-2010.

Cess, R. D., Potter, G. L., Zhang, M. H., Blanchet, J. P., Chalita, S., Colman, R., Dazlich, D. A., Del Genio, A. D., Dymnikov, V., Galin, V., Jerrett, D., Keup, E., Lacis, A. A., Le Treut, H., Liang, X. Z., Mahfouf, J. F., McAvaney, B. J., Meleshko, V. P., Mitchell, J. F. B., . . . Yagai, I. (1991, August 23). Interpretation of Snow-Climate Feedback as Produced by 17 General Circulation Models. Science, 253(5022), 888–892. https://doi.org/10.1126/science.253.5022.888.

Conway, H., Gades, A., & Raymond, C. F. (1996, June). Albedo of dirty snow during conditions of melt. Water Resources Research, 32(6), 1713–1718. https://doi.org/10.1029/96wr00712.

Cook, J. A., Tedstone, A. J., Williamson, C., McCutcheon, J., Hodson, A., Dayal, A., Skiles, S. M., Hofer, S. O., Bryant, R. G., McAree, O., McGonigle, A. J. S., Ryan, J. C., Anesio, A. M., Irvine-Fynn, T., Hubbard, A., Hanna, E., Flanner, M., Mayanna, S., Benning, L. G., . . . Tranter, M. (2020). Glacier algae accelerate melt rates on the south-western Greenland Ice Sheet. The Cryosphere, 14(1), 309–330. https://doi.org/10.5194/tc-14-309-2020.

Creamean, J. M., Suski, K. J., Rosenfeld, D., Cazorla, A., DeMott, P. J., Sullivan, R. J., White, A. B., Ralph, F. M., Minnis, P., Comstock, J. M., Tomlinson, J., & Prather, K. A. (2013). Dust and Biological Aerosols from the Sahara and Asia Influence Precipitation in the Western U.S. Science, 339(6127), 1572–1578. https://doi.org/10.1126/science.1227279.

Dang, C., & Hegg, D. A. (2014, September 10). Quantifying light absorption by organic carbon in Western North American snow by serial chemical extractions. Journal of Geophysical Research: Atmospheres, 119(17), 10,247-10,261. https://doi.org/10.1002/2014jd022156.

Davidson, C. I., Santhanam, S., Fortmann, R. C., & Marvin, P. (1985, January). Atmospheric transport and deposition of trace elements onto the Greenland Ice Sheet. Atmospheric Environment (1967), 19(12), 2065–2081. https://doi.org/10.1016/0004-6981(85)90115-5.

Di Mauro, B. (2020). A darker cryosphere in a warming world. Nature Climate Change, 10(11), 979–980. https://doi.org/10.1038/s41558-020-00911-9.

Di Mauro, B., Fava, F., Ferrero, L., Garzonio, R., Baccolo, G., Delmonte, B., & Colombo, R. (2015, June 21). Mineral dust impact on snow radiative properties in the European Alps combining ground, UAV, and satellite observations. Journal of Geophysical Research: Atmospheres, 120(12), 6080–6097. https://doi.org/10.1002/2015jd023287.

Doherty, S. J., Grenfell, T. C., Forsström, S., Hegg, D. L., Brandt, R. E., & Warren, S. G. (2013, June 6). Observed vertical redistribution of black carbon and other insoluble light-absorbing particles in melting snow. Journal of Geophysical Research: Atmospheres, 118(11), 5553–5569. https://doi.org/10.1002/jgrd.50235.

Doherty, S. J., Warren, S. G., Grenfell, T. C., Clarke, A. D., & Brandt, R. E. (2010, December 9). Light-absorbing impurities in Arctic snow. Atmospheric Chemistry and Physics, 10(23), 11647–11680. https://doi.org/10.5194/acp-10-11647-2010.

Dumka, U., Moorthy, K. K., Tripathi, S., Hegde, P., & Sagar, R. (2011, August). Altitude variation of aerosol properties over the Himalayan range inferred from spatial measurements. Journal of Atmospheric and Solar-Terrestrial Physics, 73(13), 1747–1761. https://doi.org/10.1016/j.jastp.2011.04.002.

Dumont, M., Brun, E., Picard, G., Michou, M., Libois, Q., Petit, J. R., Geyer, M., Morin, S., & Josse, B. (2014, June 8). Contribution of light-absorbing impurities in snow to Greenland's darkening since 2009 - Nature Geoscience. Nature. https://doi.org/10.1038/ngeo2180.

Eleftheriadis, K., Vratolis, S., & Nyeki, S. (2009, January). Aerosol black carbon in the European Arctic: Measurements at Zeppelin station, Ny-Ålesund, Svalbard from 1998-2007. Geophysical Research Letters, 36(2), n/a-n/a. https://doi.org/10.1029/2008gl035741.

Engvall, A. C., Ström, J., Tunved, P., Krejci, R., Schlager, H., & Minikin, A. (2009, January 1). The radiative effect of an aged, internally mixed Arctic aerosol originating from lower-latitude biomass burning. Tellus B: Chemical and Physical Meteorology, 61(4), 677. https://doi.org/10.1111/j.1600-0889.2009.00431.x.

Flanner, M., Zender, C. S., Randerson, J. T., & Rasch, P. J. (2007). Present-day climate forcing and response from black carbon in snow. Journal of Geophysical Research, 112(D11). https://doi.org/10.1029/2006jd008003.

Forsström, S., Isaksson, E., Skeie, R. B., Ström, J., Pedersen, C. A., Hudson, S. R., Berntsen, T. K., Lihavainen, H., Godtliebsen, F., & Gerland, S. (2013, December 26). Elemental carbon measurements in European Arctic snow packs. Journal of Geophysical Research: Atmospheres, 118(24), 13,614-13,627. https://doi.org/10.1002/2013jd019886.

Franzén, L. G., Mattsson, J. O., Mårtensson, U., Nihlén, T. & Rapp, A. Yellow snow over the Alps and Subarctic from dust storm in Africa, March 1991. Ambio 23, 233–235 (1994).

Gabbi, J., Huss, M., Bauder, A., Cao, F., & Schwikowski, M. (2015, July 30). The impact of Saharan dust and black carbon on albedo and long-term mass balance of an Alpine glacier. The Cryosphere, 9(4), 1385–1400. https://doi.org/10.5194/tc-9-1385-2015.

Ginoux, P., Chin, M., Tegen, I., Prospero, J. M., Holben, B., Dubovik, O., & Lin, S. J. (2001, September 1). Sources and distributions of dust aerosols simulated with the GOCART model. Journal of Geophysical Research: Atmospheres, 106(D17), 20255–20273. https://doi.org/10.1029/2000jd000053.

Graversen, R. G., & Burtu, M. (2016, May 11). Arctic amplification enhanced by latent energy transport of atmospheric planetary waves. Quarterly Journal of the Royal Meteorological Society, 142(698), 2046–2054. https://doi.org/10.1002/qj.2802.

Hansen, J. D., & Nazarenko, L. (2004). Soot climate forcing via snow and ice albedos. Proceedings of the National Academy of Sciences of the United States of America, 101(2), 423–428. https://doi.org/10.1073/pnas.2237157100.

He, C., Liou, K., Takano, Y., Yang, P., Qi, L., & Chen, F. (2018, January 24). Impact of Grain Shape and Multiple Black Carbon Internal Mixing on Snow Albedo: Parameterization and Radiative Effect Analysis. Journal of Geophysical Research: Atmospheres, 123(2), 1253–1268. https://doi.org/10.1002/2017jd027752.

Hirdman, D., Sodemann, H., Eckhardt, S., Burkhart, J. F., Jefferson, A., Mefford, T., Quinn, P. K., Sharma, S., Ström, J., & Stohl, A. (2010, January 25). Source identification of short-lived air pollutants in the Arctic using statistical analysis of measurement data and particle dispersion model output. Atmospheric Chemistry and Physics, 10(2), 669–693. https://doi.org/10.5194/acp-10-669-2010.

Horvath, H. (1993, February). Comparison of measurements of aerosol optical absorption by filter collection and a transmissometric method. Atmospheric Environment. Part a. General Topics, 27(3), 319–325. https://doi.org/10.1016/0960-1686(93)90105-8.

Huang, J., Wang, T., Wang, W., Li, Z., & Yan, H. (2014, October). Climate effects of dust aerosols over East Asian arid and semiarid regions. Journal of Geophysical Research: Atmospheres, 119(19). https://doi.org/10.1002/2014jd021796.

Huang, L., Gong, S. L., Sharma, S., Lavoué, D., & Jia, C. Q. (2010, June 4). A trajectory analysis of atmospheric transport of black carbon aerosols to Canadian high Arctic in winter and spring (1990–2005). Atmospheric Chemistry and Physics, 10(11), 5065–5073. https://doi.org/10.5194/acp-10-5065-2010.

Ikeda, K., Tanimoto, H., Sugita, T., Akiyoshi, H., Kanaya, Y., Zhu, C., & Taketani, F. (2017, September 8). Tagged tracer simulations of black carbon in the Arctic: transport, source contributions, and budget. Atmospheric Chemistry and Physics, 17(17), 10515–10533. https://doi.org/10.5194/acp-17-10515-2017.

Ingram, W. J., Wilson, C. A., & Mitchell, J. F. B. (1989, June 20). Modeling climate change: An assessment of sea ice and surface albedo feedbacks. Journal of Geophysical Research: Atmospheres, 94(D6), 8609–8622. https://doi.org/10.1029/jd094id06p08609.

IPCC, A. (2013). Climate change 2013: the physical science basis. Contribution of working group I to the fifth assessment report of the intergovernmental panel on climate change, 1535.

Jenkins, M., & Dai, A. (2021, August). The Impact of Sea-Ice Loss on Arctic Climate Feedbacks and Their Role for Arctic Amplification. Geophysical Research Letters, 48(15). https://doi.org/10.1029/2021gl094599.

Kaspari, S. D., Schwikowski, M., Gysel, M., Flanner, M. G., Kang, S., Hou, S., & Mayewski, P. A. (2011, February). Recent increase in black carbon concentrations from a Mt. Everest ice core spanning 1860-2000 AD. Geophysical Research Letters, 38(4), n/a-n/a. https://doi.org/10.1029/2010gl046096.

Kaspari, S., Painter, T. H., Gysel, M., Skiles, S. M., & Schwikowski, M. (2014, August 13). Seasonal and elevational variations of black carbon and dust in snow and ice in the Solu-Khumbu, Nepal and estimated radiative forcings. Atmospheric Chemistry and Physics, 14(15), 8089–8103. https://doi.org/10.5194/acp-14-8089-2014.

Kim, B. M., Hong, J. Y., Jun, S. Y., Zhang, X., Kwon, H., Kim, S. J., Kim, J. H., Kim, S. W., & Kim, H. K. (2017, January 4). Major cause of unprecedented Arctic warming in January 2016: Critical role of an Atlantic windstorm - Scientific Reports. Nature. https://doi.org/10.1038/srep40051.

Koch, D., & Del Genio, A. D. (2010, August 18). Black carbon semi-direct effects on cloud cover: review and synthesis. Atmospheric Chemistry and Physics, 10(16), 7685–7696. https://doi.org/10.5194/acp-10-7685-2010.

Koch, D., & Hansen, J. D. (2005). Distant origins of Arctic black carbon: A Goddard Institute for Space Studies ModelE experiment. Journal of Geophysical Research, 110(D4). https://doi.org/10.1029/2004jd005296.

Liu, D., Quennehen, B., Darbyshire, E., Allan, J. D., Williams, P. I., Taylor, J. W., Bauguitte, S. J. B., Flynn, M. J., Lowe, D., Gallagher, M. W., Bower, K. N., Choularton, T. W., & Coe, H. (2015, October 20). The importance of Asia as a source of black carbon to the European Arctic during springtime 2013. Atmospheric Chemistry and Physics, 15(20), 11537–11555. https://doi.org/10.5194/acp-15-11537-2015.

Mahowald, N. M., Kloster, S., Engelstaedter, S., Moore, J. K., Mukhopadhyay, S., McConnell, J. R., Albani, S., Doney, S. C., Bhattacharya, A., J. Curran, M. A., Flanner, M. G., Hoffman, F. M., Lawrence, D. M., Lindsay, K., Mayewski, P. A., Neff, J., Rothenberg, D., Thomas, E., Thornton, P. E., & Zender, C. S. (2010, November 19). ACP - Observed 20th century desert dust variability: impact on climate and biogeochemistry. ACP - Observed 20th Century Desert Dust Variability: Impact on Climate and Biogeochemistry. https://doi.org/10.5194/acp-10-10875-2010.

Matsui, H., Koike, M., Kondo, Y., Oshima, N., Moteki, N., Kanaya, Y., Takami, A., & Irwin, M. (2013). Seasonal variations of Asian black carbon outflow to the Pacific: Contribution from anthropogenic sources in China and biomass burning sources in Siberia and Southeast Asia. Journal of Geophysical Research: Atmospheres, 118(17), 9948–9967. https://doi.org/10.1002/jgrd.50702.

Matsui, H., Kondo, Y., Moteki, N., Takegawa, N., Sahu, L. K., Zhao, Y., Fuelberg, H. E., Sessions, W. R., Diskin, G., Blake, D. R., Wisthaler, A., & Koike, M. (2011, March 5). Seasonal variation of the transport of black carbon aerosol from the Asian continent to the Arctic during the ARCTAS aircraft campaign. Journal of Geophysical Research, 116(D5). https://doi.org/10.1029/2010jd015067.

Mattsson, Jan & Franzén, L.G. & Martensson, Ulrik & Nihlén, T. & Rapp, A.. (1994). Yellow snow over the Alps and Subarctic from dust storm in Africa. March 1991. AMBIO A Journal of the Human Environment. 23. 233-235.

McCutcheon, J., Lutz, S., Williamson, C., Cook, J. A., Tedstone, A. J., Vanderstraeten, A., Wilson, S. A., Stockdale, A., Bonneville, S., Anesio, A. M., Yallop, M. L., McQuaid, J. B., Tranter, M., & Benning, L. G. (2021b). Mineral phosphorus drives glacier algal blooms on the Greenland Ice Sheet. Nature Communications, 12(1). https://doi.org/10.1038/s41467-020-20627-w.

Meyer, T., & Wania, F. (2008, April). Organic contaminant amplification during snowmelt. Water Research, 42(8–9), 1847–1865. https://doi.org/10.1016/j.watres.2007.12.016.

Painter, T. H., Barrett, A. P., Landry, C. C., Neff, J. C., Cassidy, M. P., Lawrence, C. R., McBride, K. E., & Farmer, G. L. (2007, June 23). Impact of disturbed desert soils on duration of mountain snow cover. Geophysical Research Letters, 34(12). https://doi.org/10.1029/2007gl030284.

Painter, T. H., Skiles, S. M., Deems, J. S., Bryant, A. C., & Landry, C. C. (2012, July). Dust radiative forcing in snow of the Upper Colorado River Basin: 1. A 6 year record of energy balance, radiation, and dust concentrations. Water Resources Research, 48(7). https://doi.org/10.1029/2012wr011985.

Pedersen, C. A., Gallet, J. C., Ström, J., Gerland, S., Hudson, S. R., Forsström, S., Isaksson, E., & Berntsen, T. K. (2015, February 18). In situ observations of black carbon in snow and the corresponding spectral surface albedo reduction. Journal of Geophysical Research: Atmospheres, 120(4), 1476–1489. https://doi.org/10.1002/2014jd022407.

Pithan, F., & Mauritsen, T. (2014, February 2). Arctic amplification dominated by temperature feedbacks in contemporary climate models. Nature Geoscience, 7(3), 181–184. https://doi.org/10.1038/ngeo2071.

Polissar, A. V., Hopke, P. K., & Harris, J. M. (2001, September 26). Source Regions for Atmospheric Aerosol Measured at Barrow, Alaska. Environmental Science & Technology, 35(21), 4214–4226. https://doi.org/10.1021/es0107529.

Pöschl, U. (2003, January). Aerosol particle analysis: challenges and progress. Analytical and Bioanalytical Chemistry, 375(1), 30–32. https://doi.org/10.1007/s00216-002-1611-5.

Qi, L., & Wang, S. (2019, November). Sources of black carbon in the atmosphere and in snow in the Arctic. Science of the Total Environment, 691, 442–454. https://doi.org/10.1016/j.scitotenv.2019.07.073.

Qi, L., Li, Q., Henze, D. K., Tseng, H. L., & He, C. (2017, August 15). Sources of springtime surface black carbon in the Arctic: an adjoint analysis for April 2008. Atmospheric Chemistry and Physics, 17(15), 9697–9716. https://doi.org/10.5194/acp-17-9697-2017.

Quinn, P. K., G. Shaw, E. Andrews, E. G. Dutton, T. Ruoho-Airola, and S. L. Gong (2007), Arctic haze: Current trends and knowledge gaps, Tellus B, 59(1), 99–114, doi:10.1111/j.1600-0889.2006.00238.x.

Ramanathan, V., & Carmichael, G. R. (2008). Global and regional climate changes due to black carbon. Nature Geoscience, 1(4), 221–227. https://doi.org/10.1038/ngeo156.

Rantanen, M., Karpechko, A. Y., Lipponen, A., Nordling, K., Hyvärinen, O., Ruosteenoja, K., Vihma, T., & Laaksonen, A. (2022, August 11). The Arctic has warmed nearly four times faster than the globe since 1979 - Communications Earth & Environment. Nature. https://doi.org/10.1038/s43247-022-00498-3.

Ren, Y., Zhang, X., Wei, H., Xu, L., Zhang, J., Sun, J., Wang, X., & Li, W. (2017, March). Comparisons of methods to obtain insoluble particles in snow for transmission electron microscopy. Atmospheric Environment, 153, 61–69. https://doi.org/10.1016/j.atmosenv.2017.01.021.

Réveillet, M., Dumont, M., Gascoin, S., Lafaysse, M., Nabat, P., Ribes, A., Nheili, R., Tuzet, F., Ménégoz, M., Morin, S., Picard, G., & Ginoux, P. (2022, September 20). Black carbon and dust alter the response of mountain snow cover under climate change - Nature Communications. Nature. https://doi.org/10.1038/s41467-022-32501-y.

Reynolds, R. L., Goldstein, H. L., Moskowitz, B. M., Kokaly, R. F., Munson, S. M., Solheid, P., Breit, G. N., Lawrence, C. R., & Derry, J. (2020, April 13). Dust Deposited on Snow Cover in the San Juan Mountains, Colorado, 2011–2016: Compositional Variability Bearing on Snow-Melt Effects. Journal of Geophysical Research: Atmospheres, 125(7). https://doi.org/10.1029/2019jd032210.

Robock. (1983, April 1). Ice and Snow Feedbacks and the Latitudinal and Seasonal Distribution of Climate Sensitivity. https://journals.ametsoc.org/view/journals/atsc/40/4/1520-0469_1983_040_0986_iasfat_2_0_co_2.xml.

Ryan, J. C., Smith, L. C., van As, D., Cooley, S. W., Cooper, M. G., Pitcher, L. H., and Hubbard, A.: Greenland Ice Sheet surface melt amplified by snowline migration and bare ice exposure, Sci. Adv., 5, eaav3738, https://doi.org/10.1126/sciadv.aav3738, 2019.

Sang, J., Kim, M. K., Lau, W. K. M., & Kim, K. M. (2019, August 27). Possible Impacts of Snow Darkening Effects on the Hydrological Cycle over Western Eurasia and East Asia. Atmosphere, 10(9), 500. https://doi.org/10.3390/atmos10090500.

Schneider, S. H., & Dickinson, R. E. (1974). Climate modeling. Reviews of Geophysics, 12(3), 447. https://doi.org/10.1029/rg012i003p00447.

Schwarz, J. P., Gao, R. S., Perring, A. E., Spackman, J. R., & Fahey, D. W. (2013, March 1). Black carbon aerosol size in snow. Scientific Reports, 3(1). https://doi.org/10.1038/srep01356.

Screen, J. A., & Simmonds, I. (2010, April 1). The central role of diminishing sea ice in recent Arctic temperature amplification - Nature. Nature. https://doi.org/10.1038/nature09051.

Sellers, W. D. (1969). A Global Climatic Model Based on the Energy Balance of the Earth-Atmosphere System. AMETSOC. https://doi.org/10.1175/1520-0450(1969)008.

Sharma, S. (2004). Long-term trends of the black carbon concentrations in the Canadian Arctic. Journal of Geophysical Research, 109(D15). https://doi.org/10.1029/2003jd004331.

Shi, T., Cui, J., Chen, Y., Zhou, Y., Pu, W., Xu, X., Chen, Q., Zhang, X., & Wang, X. (2021, April 22). Enhanced light absorption and reduced snow albedo due to internally mixed mineral dust in grains of snow. Atmospheric Chemistry and Physics, 21(8), 6035–6051. https://doi.org/10.5194/acp-21-6035-2021.

Skiles, S. M., Flanner, M., Cook, J. M., Dumont, M., & Painter, T. H. (2018, October 29). Radiative forcing by light-absorbing particles in snow. Nature Climate Change, 8(11), 964–971. https://doi.org/10.1038/s41558-018-0296-5.

Sokolik, I. N., & Toon, O. B. (1996). Direct radiative forcing by anthropogenic airborne mineral aerosols. Nature, 381(6584), 681–683. https://doi.org/10.1038/381681a0.

Sterle, K. M., McConnell, J. R., Dozier, J., Edwards, R., & Flanner, M. G. (2013, February 28). Retention and radiative forcing of black carbon in eastern Sierra Nevada snow. The Cryosphere, 7(1), 365–374. https://doi.org/10.5194/tc-7-365-2013.

Stohl, A. (2006). Characteristics of atmospheric transport into the Arctic troposphere. Journal of Geophysical Research, 111(D11). https://doi.org/10.1029/2005jd006888.

Stohl, A., Berg, T., Burkhart, J. F., Fjæraa, A. M., Forster, C., Herber, A., Hov, Ø., Lunder, C. R., McMillan, W. O., Oltmans, S. J., Shiobara, M., Simpson, D., Solberg, S., Stebel, K., Ström, J., Tørseth, K., Treffeisen, R., Virkkunen, K., & Yttri, K. E. (2007). Arctic smoke – record high air pollution levels in the European Arctic due to agricultural fires in Eastern Europe in spring 2006. Atmospheric Chemistry and Physics, 7(2), 511–534. https://doi.org/10.5194/acp-7-511-2007.

Stohl, A., Klimont, Z., Eckhardt, S., Kupiainen, K., Shevchenko, V. P., Kopeikin, V. M., & Novigatsky, A. N. (2013, September 5). ACP - Black carbon in the Arctic: the underestimated role of gas flaring and residential combustion emissions. ACP - Black Carbon in the Arctic: The Underestimated Role of Gas Flaring and Residential Combustion Emissions. https://doi.org/10.5194/acp-13-8833-2013.

Stuecker, M. F., Bitz, C. M., Armour, K. C., Proistosescu, C., Kang, S. M., Xie, S. P., Kim, D., McGregor, S., Zhang, W., Zhao, S., Cai, W., Dong, Y., & Jin, F. F. (2018, November 19). Polar amplification dominated by local forcing and feedbacks - Nature Climate Change. Nature. https://doi.org/10.1038/s41558-018-0339-y.

Takeuchi, N. (2002). Optical characteristics of cryoconite (surface dust) on glaciers: the relationship between light absorbency and the property of organic matter contained in the cryoconite. Annals of Glaciology, 34, 409–414. https://doi.org/10.3189/172756402781817743.

Taylor, P. C., Cai, M., Hu, A., Meehl, J., Washington, W., & Zhang, G. J. (2013, September 9). A Decomposition of Feedback Contributions to Polar Warming Amplification. Journal of Climate, 26(18), 7023–7043. https://doi.org/10.1175/jcli-d-12-00696.1.

Tedstone, A. J., Bamber, J. L., Cook, J. M., Williamson, C. J., Fettweis, X., Hodson, A. J., & Tranter, M. (2017, November 3). Dark ice dynamics of the south-west Greenland Ice Sheet. The Cryosphere, 11(6), 2491–2506. https://doi.org/10.5194/tc-11-2491-2017.

Tegen, I., & Schepanski, K. (2018, January 20). Climate Feedback on Aerosol Emission and Atmospheric Concentrations - Current Climate Change Reports. SpringerLink. https://doi.org/10.1007/s40641-018-0086-1.

Thackeray, C. W., & Fletcher, C. G. (2016, January 6). Snow albedo feedback. Progress in Physical Geography: Earth and Environment, 40(3), 392–408. https://doi.org/10.1177/0309133315620999.

Thompson, L. G., Yao, T., Mosley-Thompson, E., Davis, M. E., Henderson, K. A., & Lin, P. N. (2000, September 15). A High-Resolution Millennial Record of the South Asian Monsoon from Himalayan Ice Cores. Science, 289(5486), 1916–1919. https://doi.org/10.1126/science.289.5486.1916.

Treffeisen, R., Tunved, P., Ström, J., Herber, A., Bareiss, J., Helbig, A., Stone, R. S., Hoyningen-Huene, W., Krejci, R., Stohl, A., & Neuber, R. (2007, June 14). Arctic smoke – aerosol characteristics during a record smoke event in the European Arctic and its radiative impact. Atmospheric Chemistry and Physics, 7(11), 3035–3053. https://doi.org/10.5194/acp-7-3035-2007.

Uecker, T. M., Kaspari, S. D., Musselman, K. N., & McKenzie Skiles, S. (2020, August 1). The Post-Wildfire Impact of Burn Severity and Age on Black Carbon Snow Deposition and Implications for Snow Water Resources, Cascade Range, Washington. Journal of Hydrometeorology, 21(8), 1777–1792. https://doi.org/10.1175/jhm-d-20-0010.1.

Van den Broeke, M. (2008, November 5). Snow and Climate: Physical Processes, Surface Energy Exchange and ModelingEdited byR.L. Armstrong & E. Brun Cambridge University Press, Cambridge, 2008 ISBN 9780521854542, 256 pages, £65. Antarctic Science, 20(6), 610–611. https://doi.org/10.1017/s0954102008001612

Wang, H., Rasch, P. J., Easter, R. C., Singh, B., Zhang, R., Ma, P., Qian, Y., Ghan, S. J., & Beagley, N. (2014, November 27). Using an explicit emission tagging method in global modeling of source-receptor relationships for black carbon in the Arctic: Variations, sources, and transport pathways. Journal of Geophysical Research: Atmospheres, 119(22). https://doi.org/10.1002/2014jd022297.

Wang, M., Xu, B. H., Cao, J., Tie, X., Wang, H., Zhang, R., Qian, Y., Rasch, P. J., Zhao, S. J., Wu, G., Zhao, H., Joswiak, D. R., Li, J., & Xie, Y. (2015b). Carbonaceous aerosols recorded in a southeastern Tibetan glacier: analysis of temporal variations and model estimates of sources and radiative forcing. Atmospheric Chemistry and Physics, 15(3), 1191–1204. https://doi.org/10.5194/acp-15-1191-2015.

Wang, X., Doherty, S. J., & Huang, J. (2013, February 11). Black carbon and other light-absorbing impurities in snow across Northern China. Journal of Geophysical Research: Atmospheres, 118(3), 1471–1492. https://doi.org/10.1029/2012jd018291.

Warneke, C., Bahreini, R., Brioude, J., Brock, C. A., de Gouw, J. A., Fahey, D. W., Froyd, K. D., Holloway, J. S., Middlebrook, A., Miller, L., Montzka, S., Murphy, D. M., Peischl, J., Ryerson, T. B., Schwarz, J. P., Spackman, J. R., & Veres, P. (2009, January). Biomass burning in Siberia and Kazakhstan as an important source for haze over the Alaskan Arctic in April 2008. Geophysical Research Letters, 36(2), n/a-n/a. https://doi.org/10.1029/2008gl036194.

Warren, S. G. (1982). Optical properties of snow. Reviews of Geophysics, 20(1), 67. https://doi.org/10.1029/rg020i001p00067.

Watson, J. G., Chow, J. C., & Chen, L. W. A. (2005). Summary of Organic and Elemental Carbon/Black Carbon Analysis Methods and Intercomparisons. Aerosol and Air Quality Research, 5(1), 65–102. https://doi.org/10.4209/aaqr.2005.06.0006.

Watson, J.G. and Chow, J.C. (2002). Comparison and evaluation of in-situ and filter carbon measurements at the Fresno Supersite. J. Geophys. Res. 107(D21):ICC 3-1-ICC 3-15.

Wexler, H. (1953, December 31). 5. RADIATION BALANCE OF THE EARTH AS A FACTOR IN CLIMATIC CHANGE. Climatic Change, 73–106. https://doi.org/10.4159/harvard.9780674367166.c5

Williamson, C. J., Cook, J., Tedstone, A., Yallop, M., McCutcheon, J., Poniecka, E., Campbell, D., Irvine-Fynn, T., McQuaid, J., Tranter, M., Perkins, R., & Anesio, A. (2020, February 24). Algal photophysiology drives darkening and melt of the Greenland Ice Sheet. Proceedings of the National Academy of Sciences, 117(11), 5694–5705. https://doi.org/10.1073/pnas.1918412117.

Wiscombe, W. J. (1980). A Model for the Spectral Albedo of Snow. I: Pure Snow. AMETSOC. https://doi.org/10.1175/1520-0469(1980)037

Xie, X., Liu, X., Che, H., Xie, X., Li, X., Shi, Z., Wang, H., Zhao, T., & Liu, Y. (2018, August 31). Radiative feedbacks of dust in snow over eastern Asia in CAM4-BAM. Atmospheric Chemistry and Physics, 18(17), 12683–12698. https://doi.org/10.5194/acp-18-12683-2018.

Xu, B., Cao, J., Hansen, J., Yao, T., Joswia, D. R., Wang, N., Wu, G., Wang, M., Zhao, H., Yang, W., Liu, X., & He, J. (2009, December 29). Black soot and the survival of Tibetan glaciers. Proceedings of the National Academy of Sciences, 106(52), 22114–22118. https://doi.org/10.1073/pnas.0910444106.

Xu, B., Cao, J., Joswiak, D. R., Liu, X., Zhao, H., & He, J. (2012, February 22). Post-depositional enrichment of black soot in snow-pack and accelerated melting of Tibetan glaciers. Environmental Research Letters, 7(1), 014022. https://doi.org/10.1088/1748-9326/7/1/014022.

Xu, J. W., Martin, R. V., Morrow, A., Sharma, S., Huang, L., Leaitch, W. R., Burkart, J., Schulz, H., Zanatta, M., Willis, M. D., Henze, D. K., Lee, C. J., Herber, A. B., & Abbatt, J. P. D. (2017, October 10). Source attribution of Arctic black carbon constrained by aircraft and surface measurements. Atmospheric Chemistry and Physics, 17(19), 11971–11989. https://doi.org/10.5194/acp-17-11971-2017.